Smart Control of Guest Inclusion with α-Cyclodextrin Using its Hydration History

Askar K. Gatiatulin, Viktoria Yu. Osel'skaya, Marat A. Ziganshin, Valery V. Gorbatchuk*

A. M. Butlerov Institute of Chemistry, Kazan Federal University, Kremlyovskaya 18, 420008 Kazan, Russia

Corresponding Author: Prof. Valery V.Gorbatchuk A.M. Butlerov Institute of Chemistry, Kazan Federal University, Kremlevskaya 18, 420008 Kazan, Russia, Fax: +7 843 2927418. Tel: +7 843 2337309. E-mail: Valery.Gorbatchuk@kpfu.ru.

Electronic Supplementary Material

## TG/MS curves for clathrates prepared with saturation of aCD·5.9H₂O hexahydrate

Figure S1. Product of saturation of aCD·5.9H$_2$O hexahydrate with benzene vapor (no benzene inclusion).

Figure S2. Product of saturation of aCD·5.9H$_2$O hexahydrate with MeOH vapor: aCD·2.2CH$_3$OH·2.3H$_2$O.
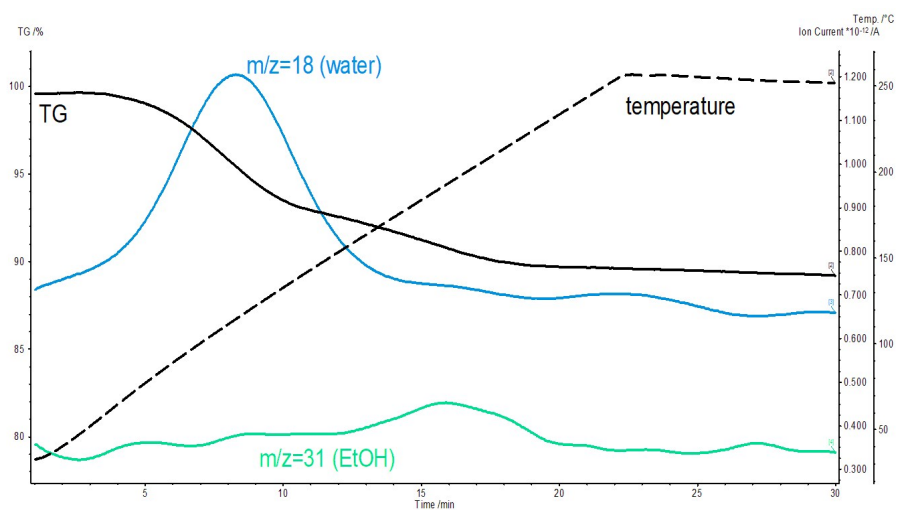
Figure S3. Product of saturation of aCD·5.9H$_2$O hexahydrate with EtOH vapor: aCD·1.0EtOH·3.5H$_2$O.
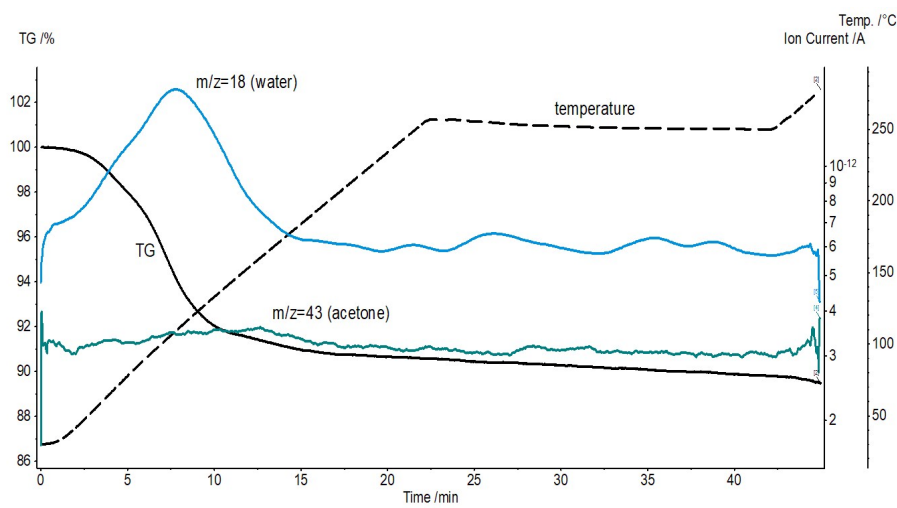
Figure S4. Product of saturation of aCD·5.9H$_2$O hexahydrate with acetone vapor: aCD·0.2(CH$_3$)$_2$CO·3.5H$_2$O
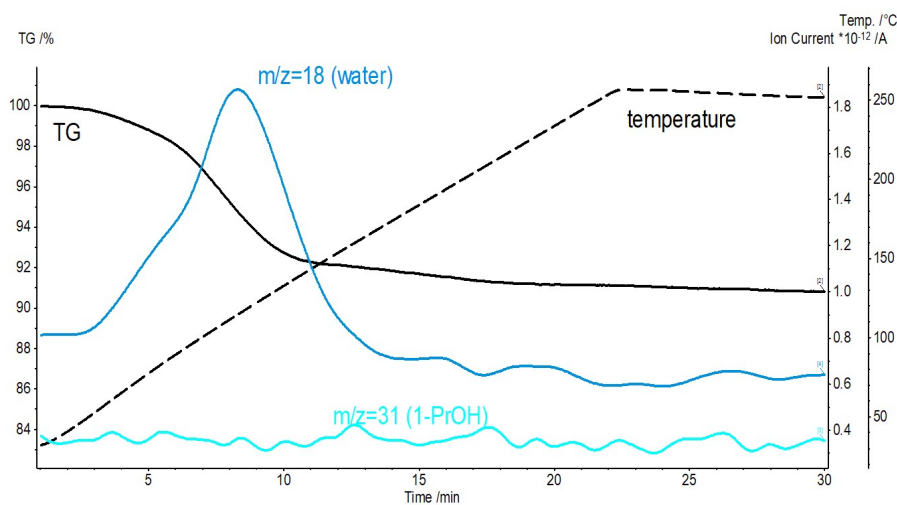
Figure S5. Product of saturation of aCD·5.9H$_2$O hexahydrate with n-PrOH vapor: aCD·0.3n-PrOH·5H$_2$O
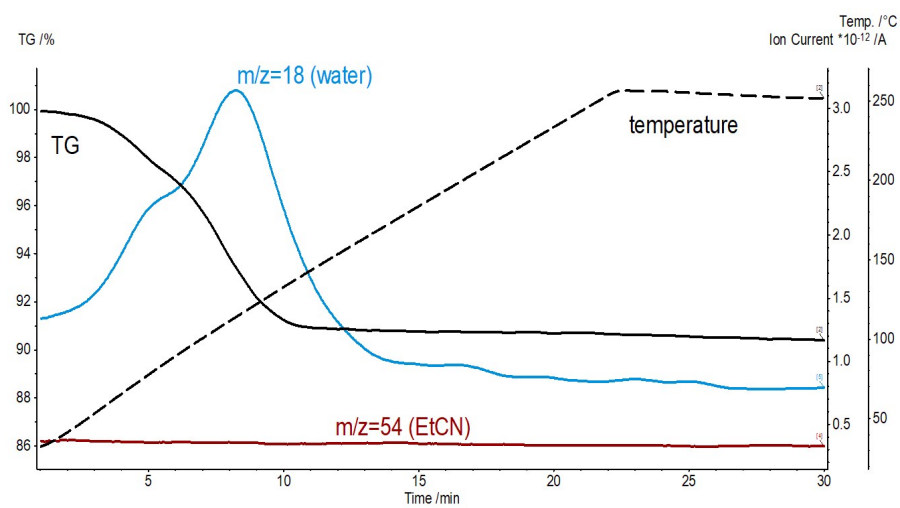
Figure S6. Product of saturation of aCD·5.9H$_2$O hexahydrate with benzene EtCN vapor (no EtCN inclusion).
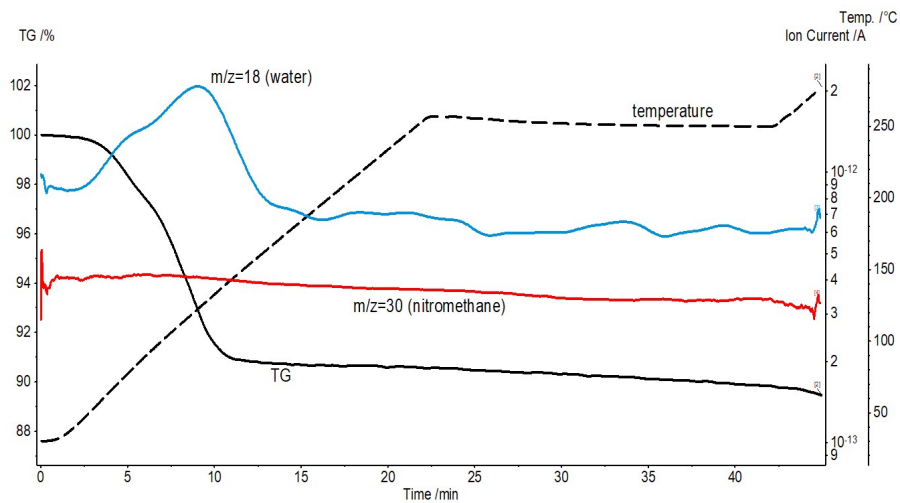
Figure S7. Product of saturation of aCD·5.9H$_2$O hexahydrate with nitromethane vapor (no nitromethane inclusion).

TG/MS curves for clathrates prepared with saturation of tetrahydrate A
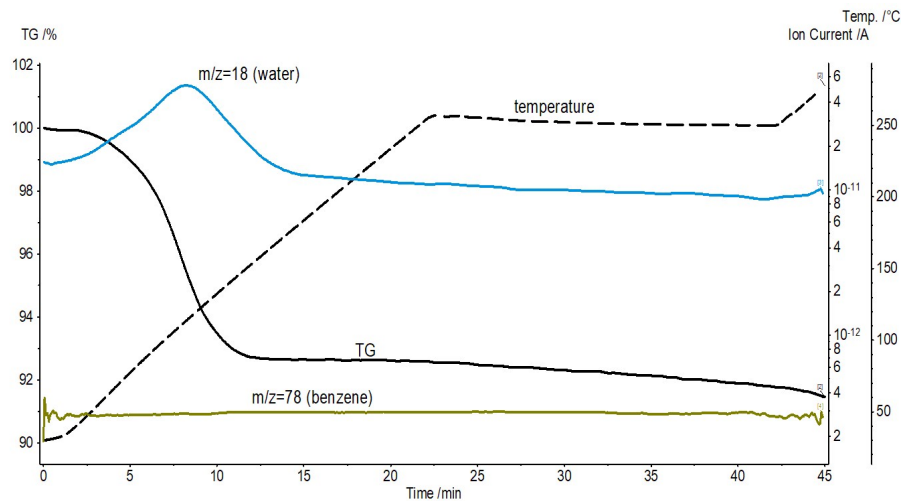
Figure S8. Product of saturation of aCD tetrahydrate **A** with benzene vapor (no benzene inclusion).
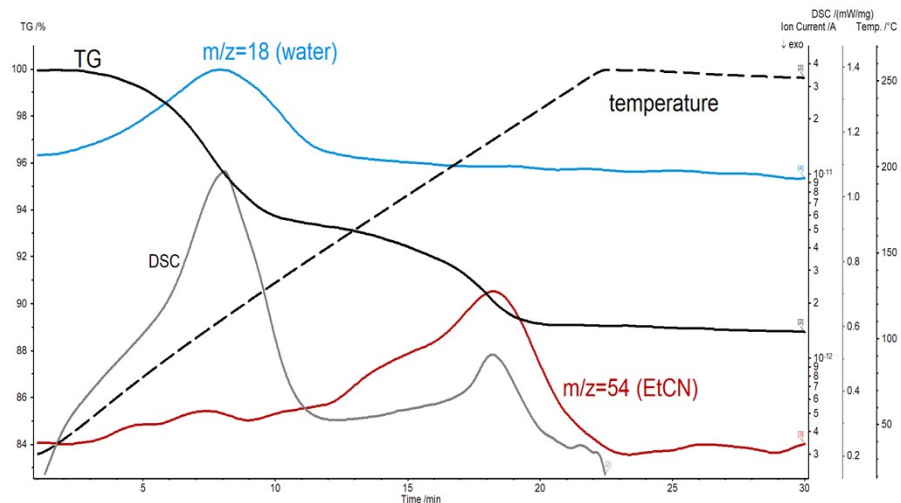
Figure S9. Product of saturation of aCD tetrahydrate **A** with EtCN vapor (aCD·0.9EtCN·3.8H$_2$O).
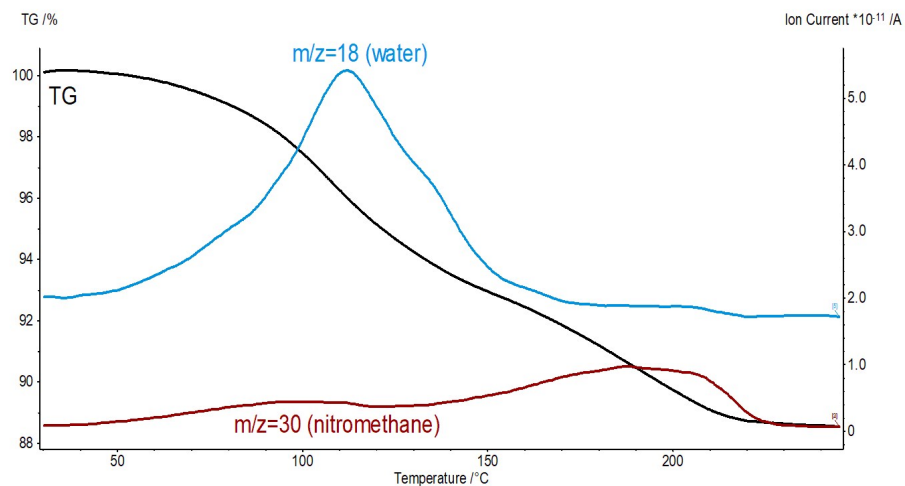
Figure S10. Product of saturation of aCD tetrahydrate **A** with nitromethane vapor (aCD·1.4MeNO$_2$·2.0H$_2$O).
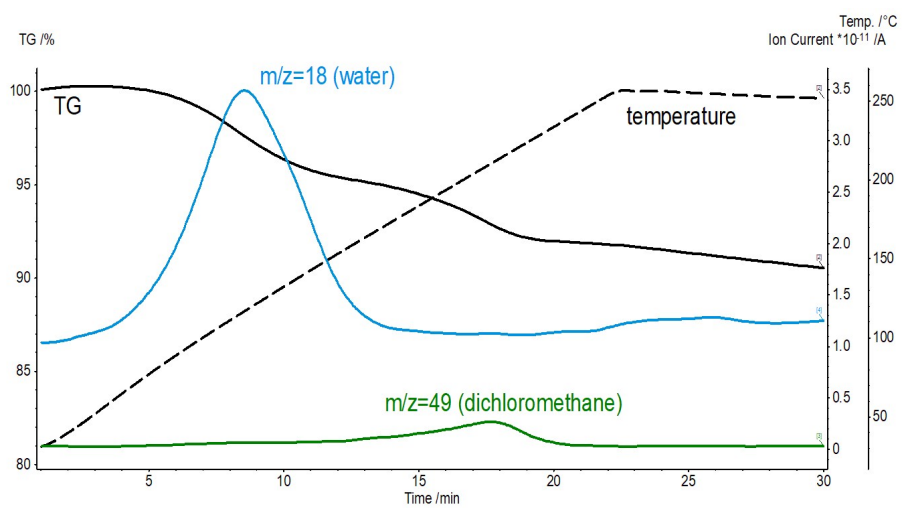
Figure S11. Product of saturation of aCD tetrahydrate **A** with dichloromethane vapor (aCD·0.4CH$_2$Cl$_2$·3.0H$_2$O).
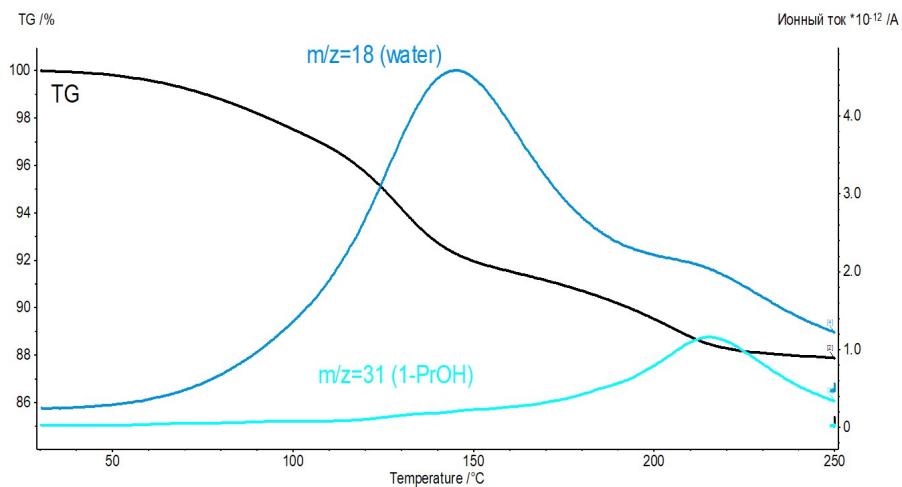
Figure S12. Product of saturation of aCD tetrahydrate **A** with n-PrOH vapor (aCD·0.9*n*-PrOH·4.3H$_2$O).
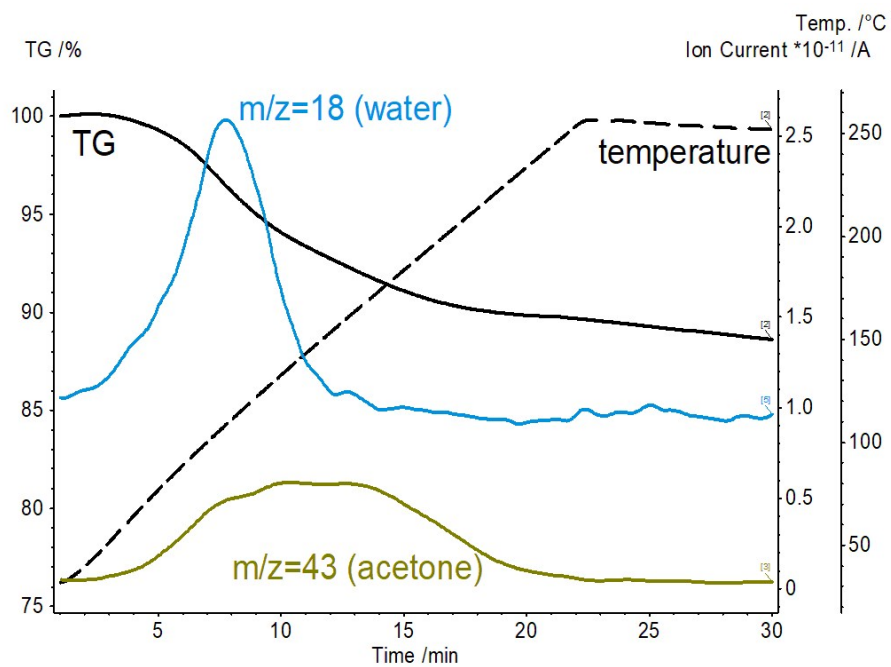
Figure S13. Product of saturation of aCD tetrahydrate **A** with acetone vapor (aCD·1.2(CH$_3$)$_2$CO·2.3H$_2$O).

## TG/MS curves for clathrates with saturation of tetrahydrate B
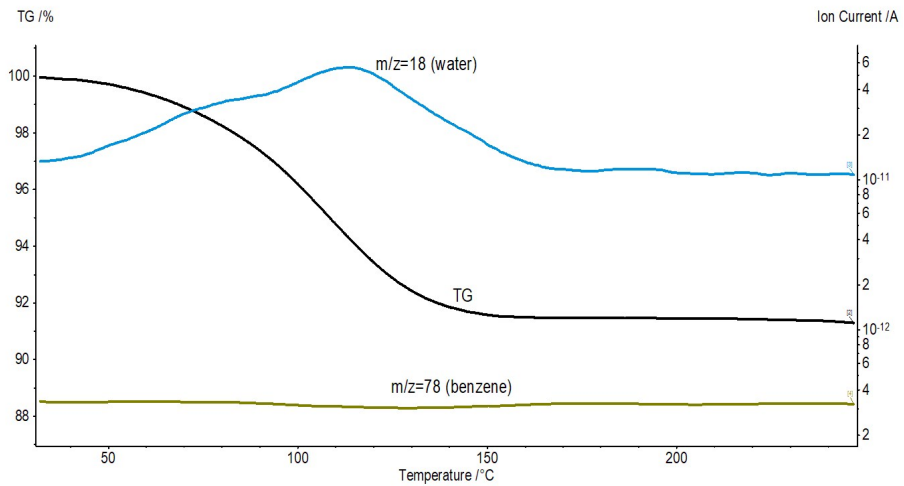
Figure S14. Product of saturation of aCD tetrahydrate **B** with benzene vapor (no benzene inclusion).
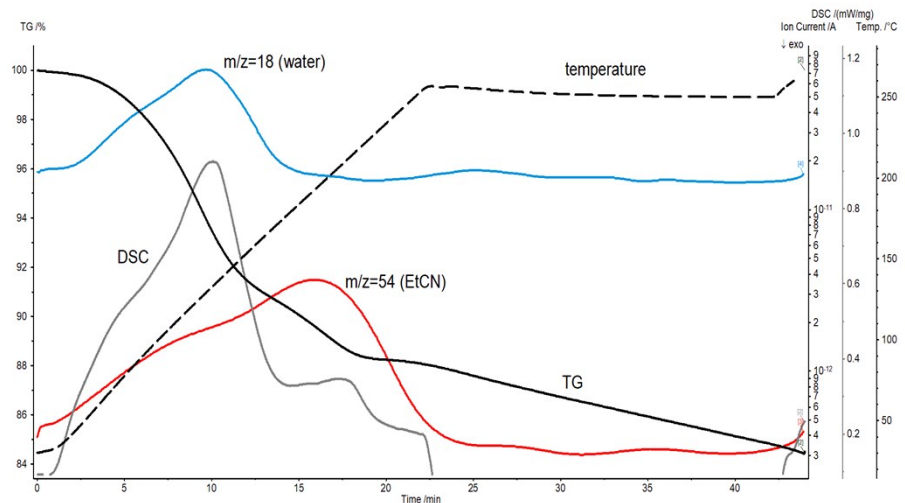
Figure S15. Product of saturation of aCD tetrahydrate **B** with EtCN vapor (aCD·1.0EtCN·4.1H$_2$O).
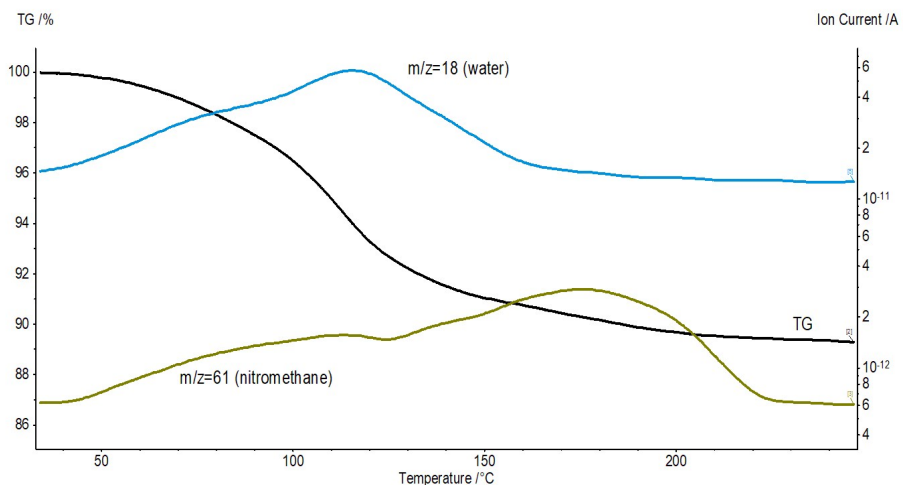
Figure S16. Product of saturation of aCD tetrahydrate **B** with nitromethane vapor (aCD·0.6MeNO$_2$·4.5H$_2$O).
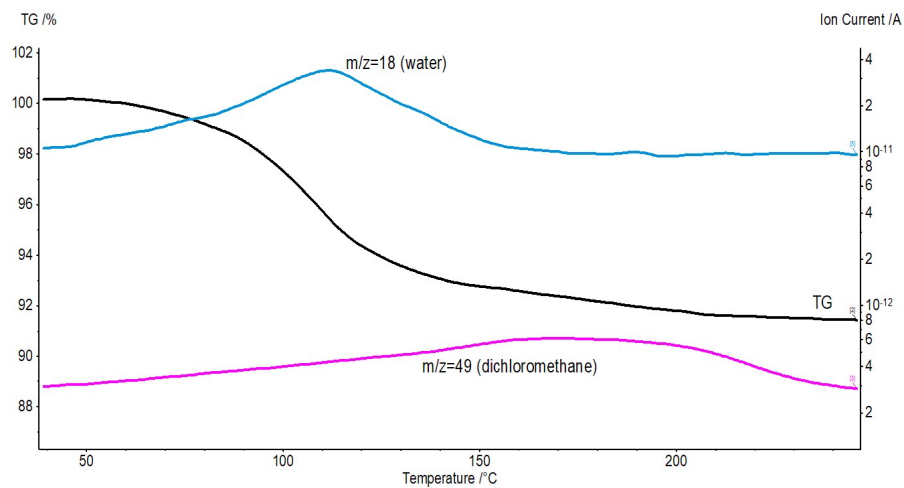
Figure S17. Product of saturation of aCD tetrahydrate **B** with dichloromethane vapor (aCD·0.3CH$_2$Cl$_2$·4.0H$_2$O).
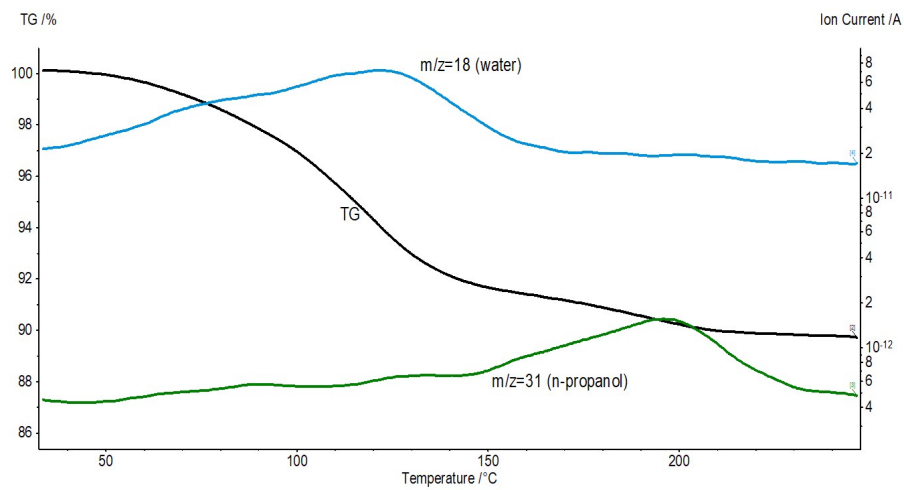
Figure S18. Product of saturation of aCD tetrahydrate **B** with *n*-propanol vapor (aCD·0.5*n*-PrOH·4.7H$_2$O).
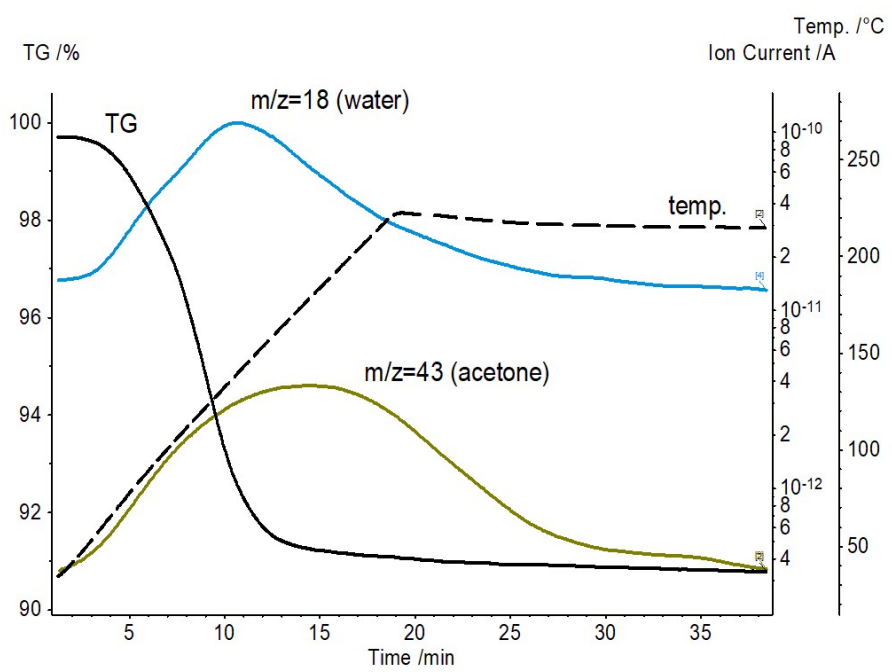
Figure S19. Product of saturation of aCD tetrahydrate **B** with acetone vapor (aCD·0.3(CH$_3$)$_2$CO·4.0H$_2$O).

TG/MS curves for clathrates prepared with saturation of hexahydrate aCD·5.9H$_2$O in the presence of a desiccant
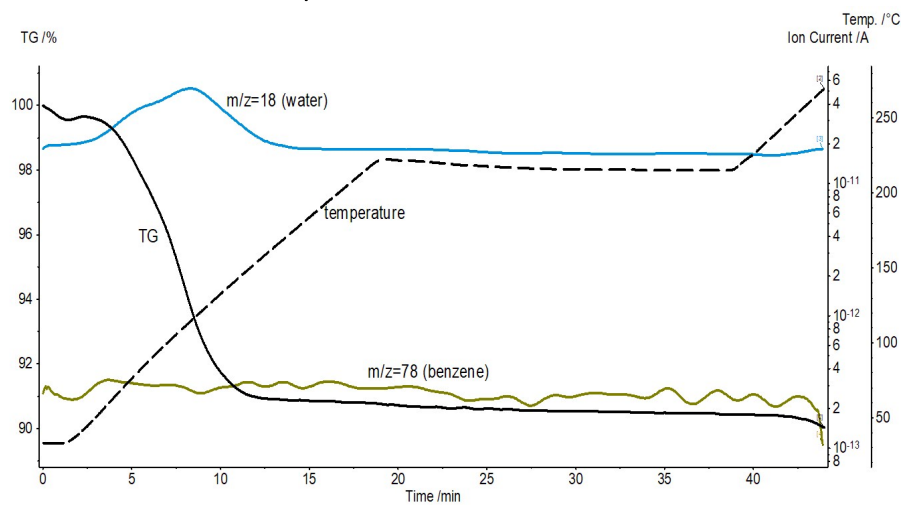
Figure S20. Product of saturation of aCD·5.9H$_2$O hexahydrate with benzene vapor in the presence of a desiccant (no benzene inclusion).
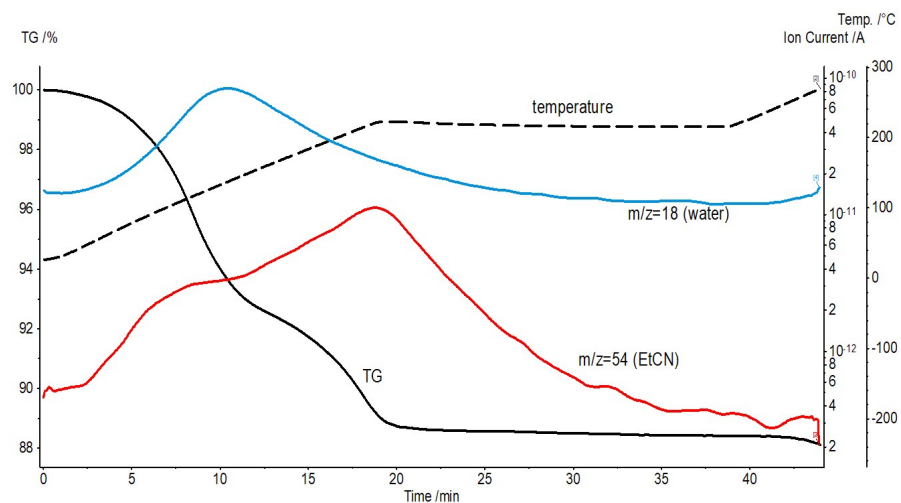
Figure S21. Product of saturation of aCD·5.9H$_2$O hexahydrate with EtCN vapor in the presence of a desiccant (aCD·1.1EtCN·3.6H$_2$O).
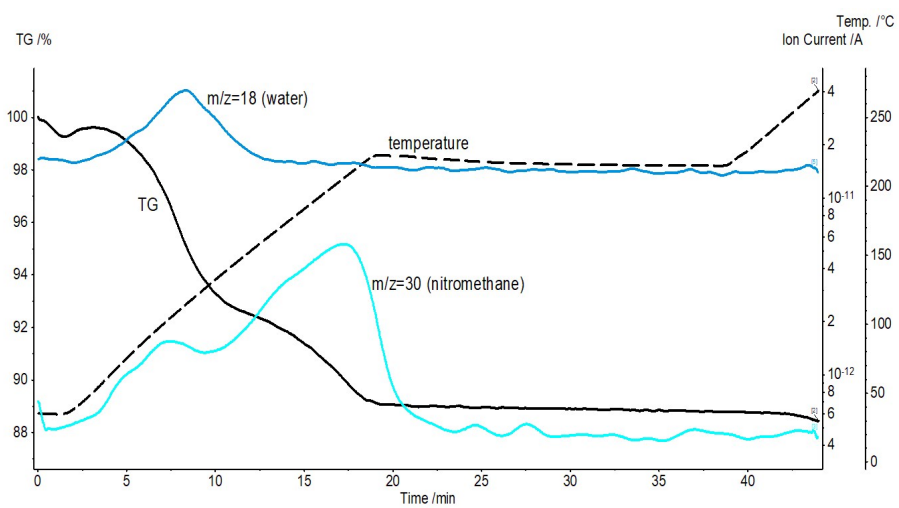
Figure S22. Product of saturation of aCD·5.9H$_2$O hexahydrate with nitromethane vapor in the presence of a desiccant (aCD·1.0MeNO$_2$·3.0H$_2$O).
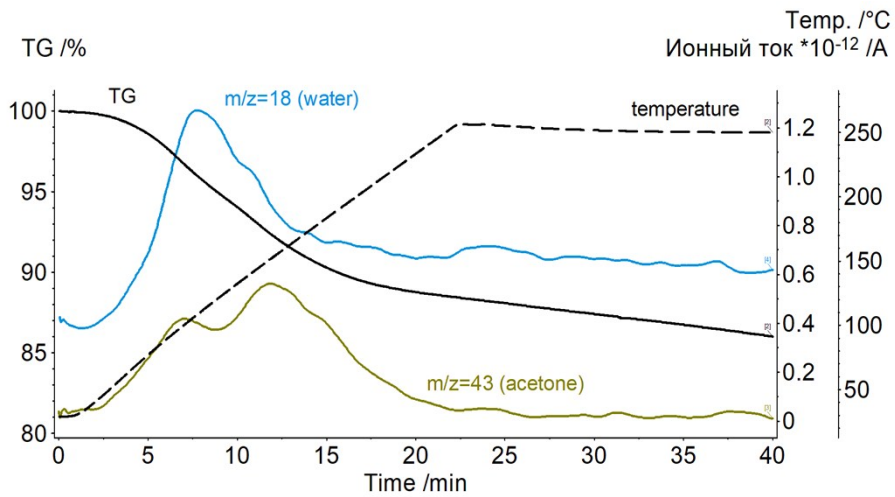
Figure S23. Product of saturation of aCD·5.9H$_2$O hexahydrate with acetone vapor in the presence of a desiccant (aCD·1.3(CH$_3$)$_2$CO·2.7H$_2$O).
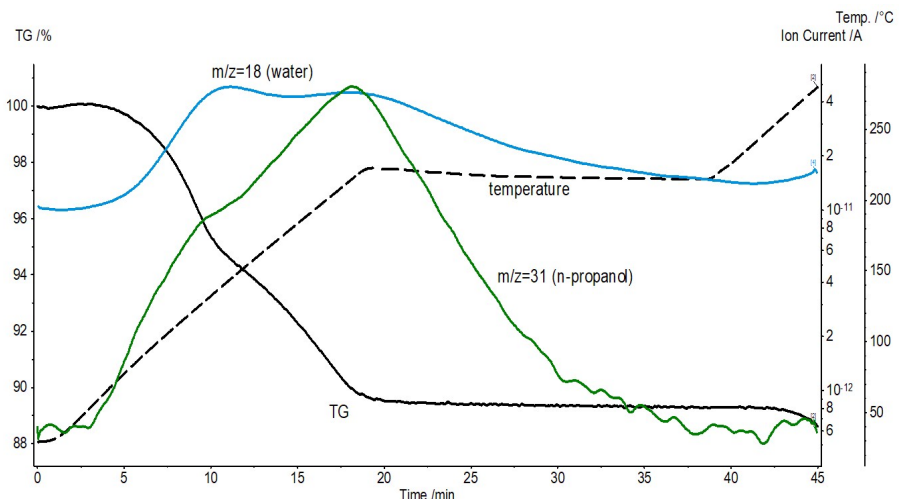
Figure S24. Product of saturation of aCD·5.9H$_2$O hexahydrate with n-propanol vapor in the presence of a desiccant (aCD·1.1n-PrOH·3.0H$_2$O).

TG/DSC/MS curves for the tetrahydrate B and ternary clathrates with EtCN
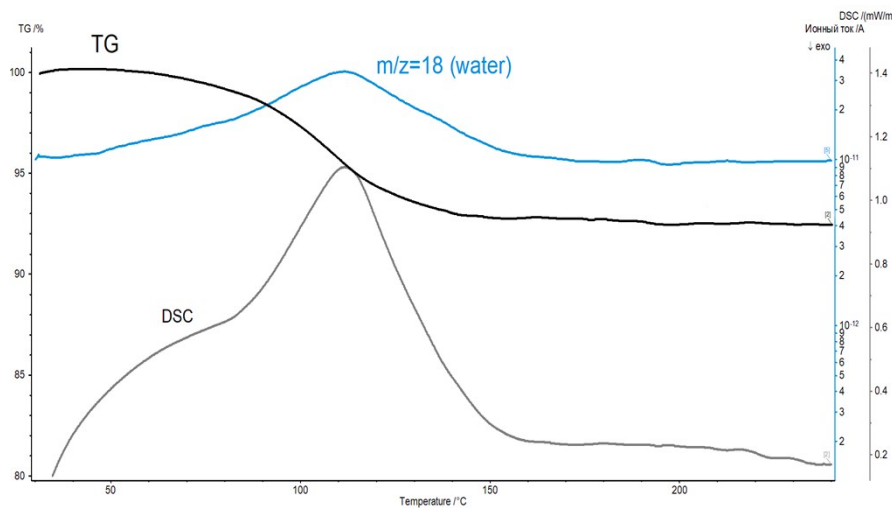
Figure S25. Tetrahydrate **B**.
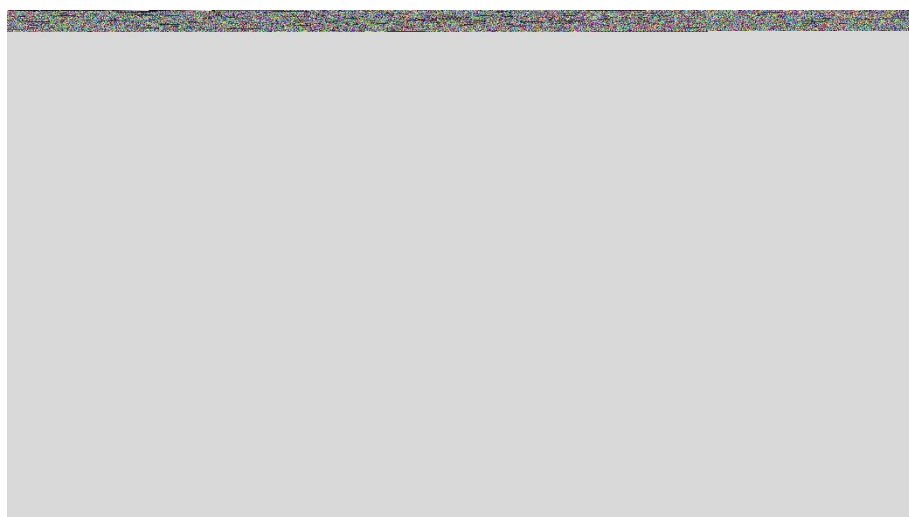
Figure S26. Product of saturation of aCD tetrahydrate **A** with EtCN vapor (aCD·0.9EtCN·3.8H$_2$O).
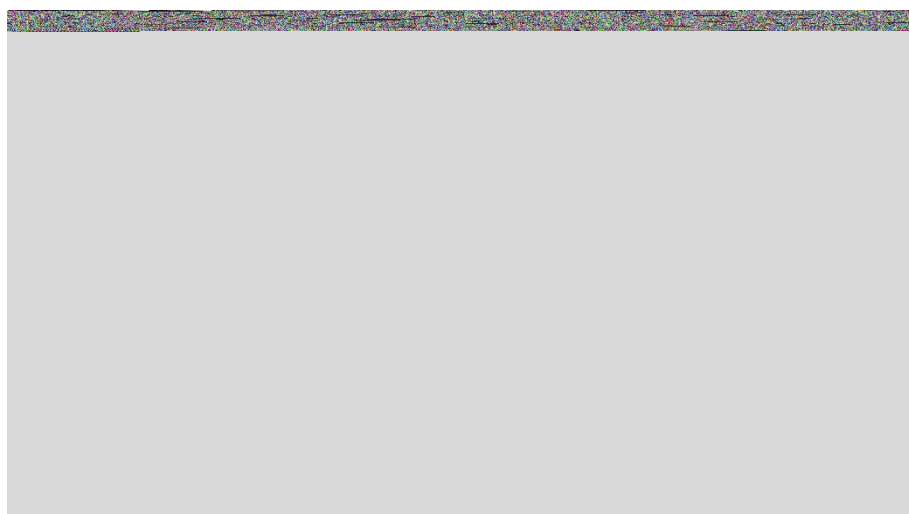
Figure S27. Product of saturation of aCD tetrahydrate **B** with EtCN vapor (aCD·1.0EtCN·4.1H$_2$O).

X-Ray powder diffraction data

Table S1. PXRD data table for tetrahydrate **A** (Form **IIIa**).

peak No.	2θ (°)	d(Å)	Height(counts)	FWHM(°)	Relative intensity (%)	Asym. factor
1	4.919	17.5354	1726.9	0.2103	16.54	2.5985
2	6.537	13.2886	146.9	0.2544	1.47	0.9218
3	9.534	9.1860	3221.9	0.2963	35.80	1.1518
4	9.816	8.9277	790.8	0.1656	4.91	0.5654
5	12.179	7.2321	4230.6	0.4557	82.51	4.8649
6	12.488	7.0576	479.6	0.4001	10.70	0.4626
7	13.322	6.6267	4204.5	0.4817	100.00	0.589
8	13.765	6.4196	2233.8	0.2206	20.21	4.3998
9	14.798	5.9839	796.5	0.2893	8.64	1.1502
10	15.640	5.6716	1003.6	0.3215	12.10	1.1605
11	16.057	5.5292	532.2	0.2775	5.54	0.7593
12	16.574	5.3627	105.1	0.2553	1.01	2.793
13	18.271	4.8827	1348.0	0.6622	56.05	0.4539
14	19.742	4.5342	1446.6	0.3135	21.48	2.7261
15	20.130	4.4508	521.4	0.3944	13.45	0.3169
16	20.651	4.3440	250.9	0.2272	3.36	0.7104
17	21.153	4.2461	493.4	0.5548	16.27	0.6762
18	21.919	4.1054	2705.7	0.3901	56.82	1.2509
19	22.903	3.9390	486.8	0.6161	19.72	0.3015
20	24.031	3.7653	97.3	0.0865	0.45	1.325
21	24.786	3.6581	195.6	0.518	5.80	0.8652
22	25.547	3.5568	561.7	0.323	7.98	4.6633
23	26.486	3.4399	557.0	0.2881	6.95	1.1155
24	26.994	3.3801	589.4	0.5197	13.58	0.8013
25	28.056	3.2626	257.4	0.2921	3.41	0.5635
26	29.058	3.1600	366.0	0.6388	9.78	1.842
27	30.492	3.0253	325.3	0.442	5.96	2.1048
28	31.212	2.9626	580.6	0.8652	23.03	0.474
29	33.061	2.8149	519.6	0.401	9.16	0.8974
30	33.781	2.7620	526.4	0.3853	8.56	1.6299
31	34.572	2.7067	542.4	0.4945	11.54	1.2261
32	36.048	2.6104	267.5	0.3383	4.18	0.6361
33	36.964	2.5549	301.1	0.41	5.65	1.2618
34	38.187	2.4853	251.2	0.3486	4.07	0.4315
35	39.868	2.3973	189.4	3.6532	27.37	4.997

Table S2. PXRD data table for tetrahydrate **B** (Form **I**).

peak No.	2θ (°)	d(Å)	Height(counts)	FWHM(°)	Relative intensity (%)	Asym. factor
1	5.011	17.6370	433.1	0.239	5.79	2.8157
2	6.115	14.4622	36.2	0.4688	0.83	0.5924
3	9.436	9.3968	1177.4	0.3417	16.60	0.9891
4	10.479	8.4703	236.0	0.3196	3.16	3.3676
5	11.663	7.6208	1243.7	0.6654	47.49	0.3172
6	11.961	7.4339	3455.8	0.3161	53.28	4.8725
7	13.294	6.6998	2538.2	0.331	39.50	1.7058
8	14.115	6.3175	3346.9	0.2831	41.31	4.3347
9	14.975	5.9621	1087.0	0.2962	14.27	3.4181
10	15.683	5.6992	1344.5	0.4593	27.16	3.804
11	16.841	5.3175	391.3	0.2541	3.99	1.4678
12	17.881	5.0177	979.7	0.5946	25.90	0.4803
13	18.591	4.8323	1049.1	0.7771	36.40	0.4159
14	18.930	4.7488	1240.4	0.2362	12.77	0.8932
15	19.376	4.6435	1120.3	0.2904	13.75	2.3164
16	19.718	4.5662	1279.3	0.4304	24.21	0.6884
17	19.917	4.5224	921.6	2.3907	100.00	0.2032
18	21.503	4.2029	4711.5	0.328	64.77	3.1223
19	21.992	4.1141	1761.5	0.3896	28.96	2.4226
20	22.575	4.0131	1574.4	0.2823	18.82	2.1531
21	23.391	3.8806	1233.4	0.381	20.31	1.1631
22	23.862	3.8084	763.0	0.4022	12.79	3.9144
23	24.180	3.7612	561.0	0.4187	9.74	4.9863
24	25.443	3.5860	739.9	0.5201	16.43	1.6631
25	27.110	3.3807	1041.3	0.5779	24.95	5
26	27.642	3.3206	538.3	0.5944	13.84	1.1222
27	28.543	3.2243	467.8	0.3045	6.04	2.041
28	29.022	3.1756	532.0	0.3496	7.71	4.9953
29	30.069	3.0748	641.2	0.316	8.52	2.716
30	30.434	3.0414	662.6	0.4735	13.64	0.9742
31	30.852	3.0042	589.4	0.2417	6.17	1.0997
32	31.542	2.9450	455.7	0.8012	16.26	0.4529
33	33.109	2.8204	662.8	0.693	19.05	4.9857
34	34.194	2.7413	300.4	0.5967	7.80	0.9489
35	34.956	2.6889	904.9	0.5208	20.47	0.9966
36	36.007	2.6206	281.5	0.4552	5.57	0.9633
37	36.916	2.5649	674.9	0.8842	26.28	0.6568
38	38.479	2.4760	643.7	0.6355	17.34	2.071
39	39.484	2.4229	569.8	0.5195	12.84	1.025
40	40.949	2.3507	215.1	0.2978	2.73	1.8055
41	41.751	2.3136	181.0	0.7449	5.63	3.4609
42	42.477	2.2814	174.2	0.666	4.93	1.9006

Table S3. PXRD data table for aCD·1.3(CH$_3$)$_2$CO·2.7H$_2$O clathrate prepared in "hexahydrate+desiccant+guest" system (columnar packing type).

peak No.	2θ (°)	d(Å)	Height(counts)	FWHM(°)	Relative intensity (%)	Asym. factor
1	5.692	15.5338	202.8	0.3204	3.07	1.2243
2	7.451	11.8800	1932.3	0.3081	29.56	1.3056
3	9.664	9.1778	170.8	0.3959	3.57	3.2849
4	11.470	7.7474	710.9	0.5855	28.26	0.6397
5	12.989	6.8542	2058.8	0.4621	52.69	2.3407
6	14.914	5.9862	418.0	0.5081	10.38	1.9101
7	16.164	5.5341	356.4	0.6917	12.09	1.8234
8	17.126	5.2316	202.7	0.5312	5.63	0.8144
9	18.408	4.8788	246.3	7.1875	100.00	0.2476
10	19.845	4.5382	3240.4	0.4965	80.19	1.4838
11	22.512	4.0237	591.4	1.0086	28.92	2.1096
12	27.075	3.3848	210.0	0.7638	8.00	0.7067
14	33.667	2.7790	132.7	2.064	11.82	0.7339

Table S4. PXRD data table for aCD·1.1EtCN·3.6H$_2$O clathrate prepared in "hexahydrate+desiccant+guest" system (Form **III** packing type).

| peak No.	2θ (°)	d(Å)	Height(counts)	FWHM(°)	Relative intensity (%)	Asym. factor
1	4.693	18.8145	622.5	0.2244	12.6	1.4836
2	6.743	13.0991	121.0	0.3125	2.5	2.9897
3	8.014	11.0236	194.8	0.4374	5.9	3.6165
4	9.398	9.4026	934.2	0.2643	16.4	1.7307
5	9.627	9.1799	1070.7	0.281	20.2	0.959
6	10.468	8.4442	243.4	0.2053	3.2	1.4706
7	11.712	7.5495	2481.2	0.2871	49.2	2.1308
8	12.225	7.2342	1339.9	0.8305	84.1	0.2518
9	12.547	7.0493	1973.4	0.2026	27.9	1.7335
10	13.294	6.6547	4389.4	0.3285	100.0	1.9593
11	13.705	6.4559	647.7	0.2485	11.2	1.9837
12	14.684	6.0277	1059.4	0.2932	21.5	2.0316
13	15.564	5.6889	330.8	0.4144	12.2	0.5476
14	16.339	5.4207	639.7	0.4253	19.5	4.9811
15	17.031	5.2020	315.3	0.5264	14.5	0.6545
16	17.678	5.0131	360.6	0.2259	6.5	1.6164
17	18.185	4.8745	1231.7	0.3709	37.2	1.2991
18	18.961	4.6765	906.9	0.3064	21.8	1.8611
19	19.612	4.5229	1796.2	0.4911	70.8	1.461
20	20.079	4.4188	1571.5	0.3228	40.2	1.6421
21	21.108	4.2056	1111.8	0.3829	33.7	1.658
22	21.615	4.1080	931.9	0.3834	26.1	3.9454
23	22.247	3.9928	4017.2	0.4685	139.6	3.2879
24	23.138	3.8410	1290.7	0.7091	73.5	1.463
25	24.643	3.6098	231.3	0.4499	8.6	1.1261
26	25.522	3.4874	650.7	0.3749	17.5	4.9323
27	26.213	3.3970	92.7	0.2041	1.8	0.2803
28	26.905	3.3112	382.1	0.3655	11.3	1.3058
29	27.797	3.2068	388.3	0.4515	15.0	0.8041
30	28.463	3.1333	423.0	0.3488	11.6	1.7515
31	29.140	3.0620	353.4	0.297	8.6	1.182
32	30.574	2.9216	259.9	0.5498	11.4	1.5737
33	31.222	2.8625	488.5	0.7436	32.6	0.4897
34	33.045	2.7086	518.8	0.4298	16.6	3.2194
35	34.418	2.6036	343.4	1.2004	32.0	2.0452
36	37.122	2.4199	181.0	0.257	3.3	5
37	38.334	2.3462	150.2	0.1883	2.4	2.2309
38	39.544	2.2771	235.8	0.9469	19.6	1.8003

X-Ray powder diffractograms
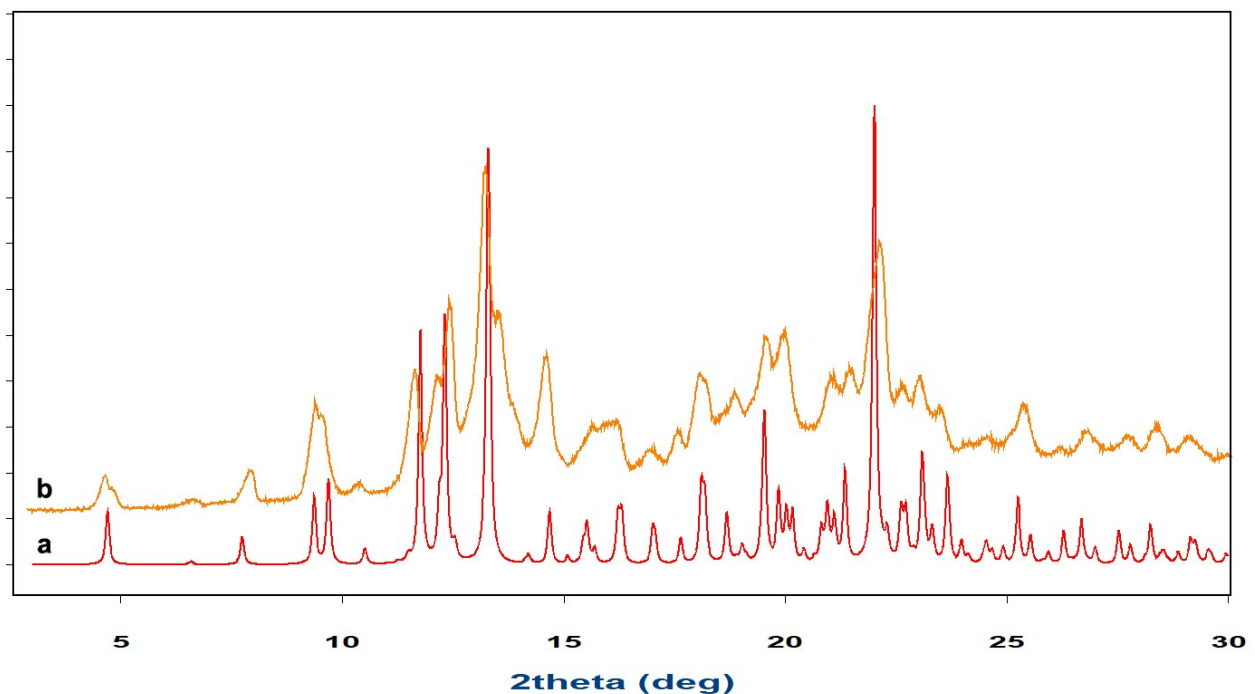
Figure S28. Powder diffractograms for: (a) aCD·7.57H_2O hydrate (Form **III**) simulated from single crystal XRD data[1]; (b) aCD·0.9EtCN·3.8H_2O prepared from tetrahydrate **A**.
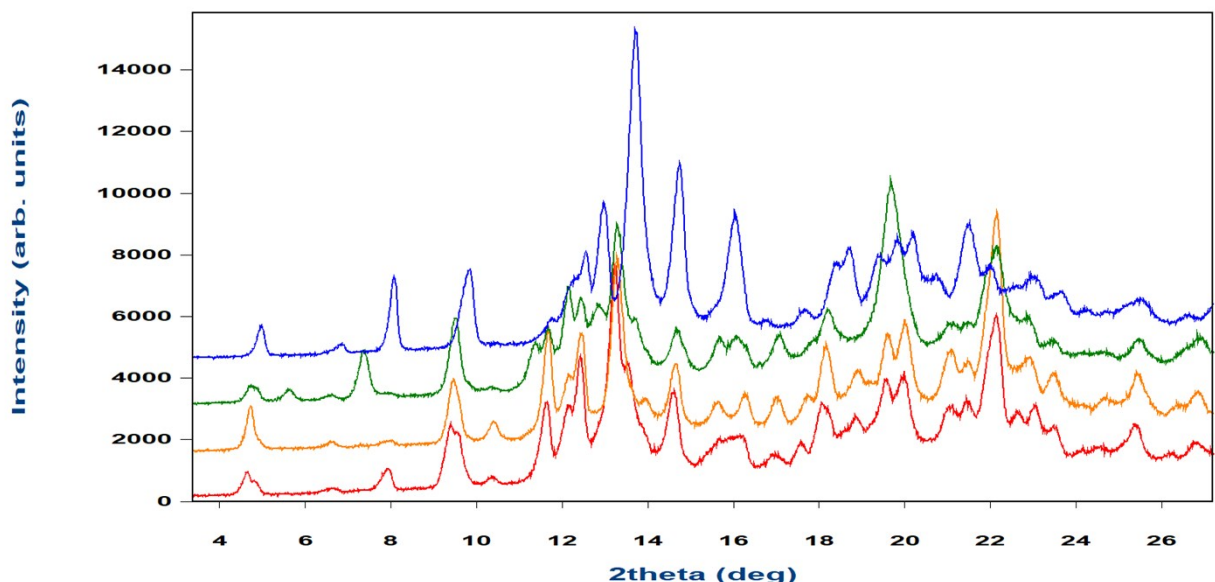

Figure S29. Powder diffractograms for clathrates prepared from aCD tetrahydrate **A**: (red) aCD·0.9C_2H_5CN·3.8H_2O; (orange) aCD·1.4CH_3NO_2·2.0H_2O; (green) aCD·1.2$(CH_3)_2CO$·2.3H_2O; (blue) aCD·0.4CH_2Cl_2·3.0H_2O.
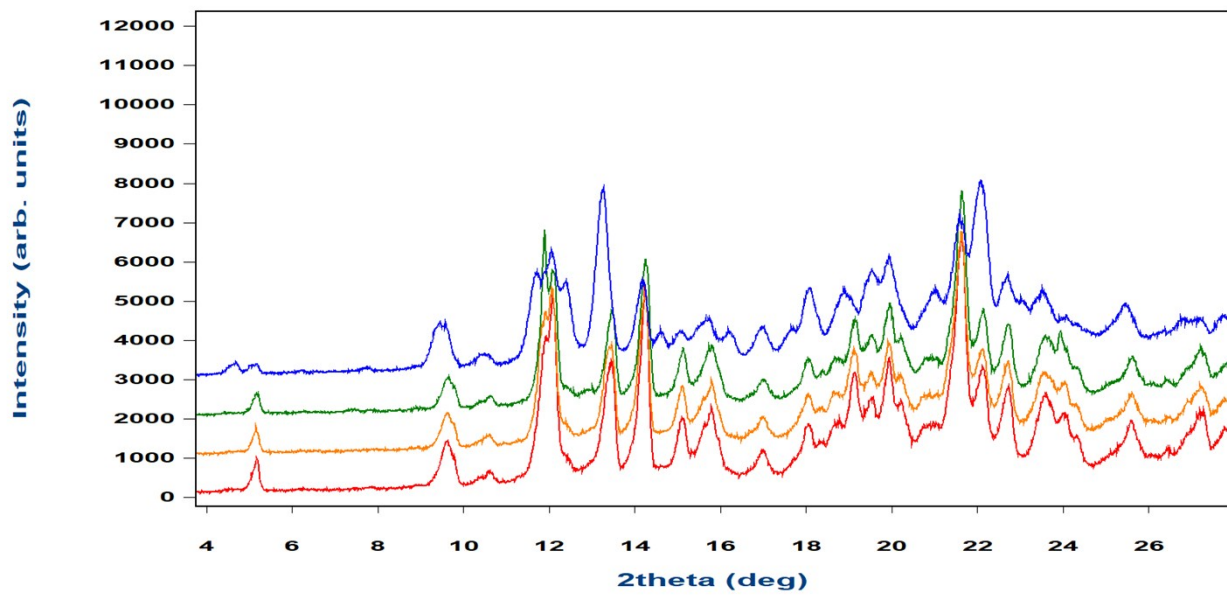
Figure S30. Powder diffractograms for clathrates prepared from aCD tetrahydrate **B**: (red) aCD·0.5n-C$_3$H$_7$OH·4.7H$_2$O; (orange) aCD·0.3CH$_2$Cl$_2$·4.0H$_2$O; (green) aCD·0.3(CH$_3$)$_2$CO·4.0H$_2$O; (blue) aCD·1.0C$_2$H$_5$CN·4.1H$_2$O.
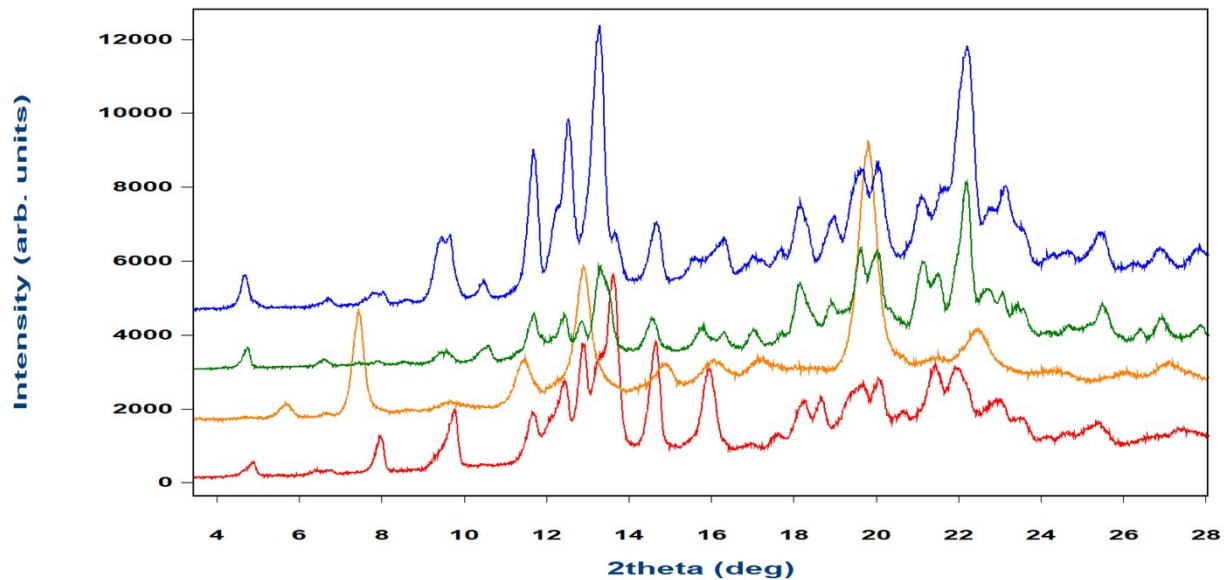

Figure S31. Powder diffractograms for aCD clathrates prepared in "hexahydrate+desiccant+guest" system: (red) aCD·1.1n-C$_3$H$_7$OH·3.0H$_2$O; (orange) aCD·1.3(CH$_3$)$_2$CO·2.7H$_2$O; (green) aCD·1.0CH$_2$Cl$_2$·2.0H$_2$O; (blue) aCD·1.1C$_2$H$_5$CN·3.6H$_2$O.
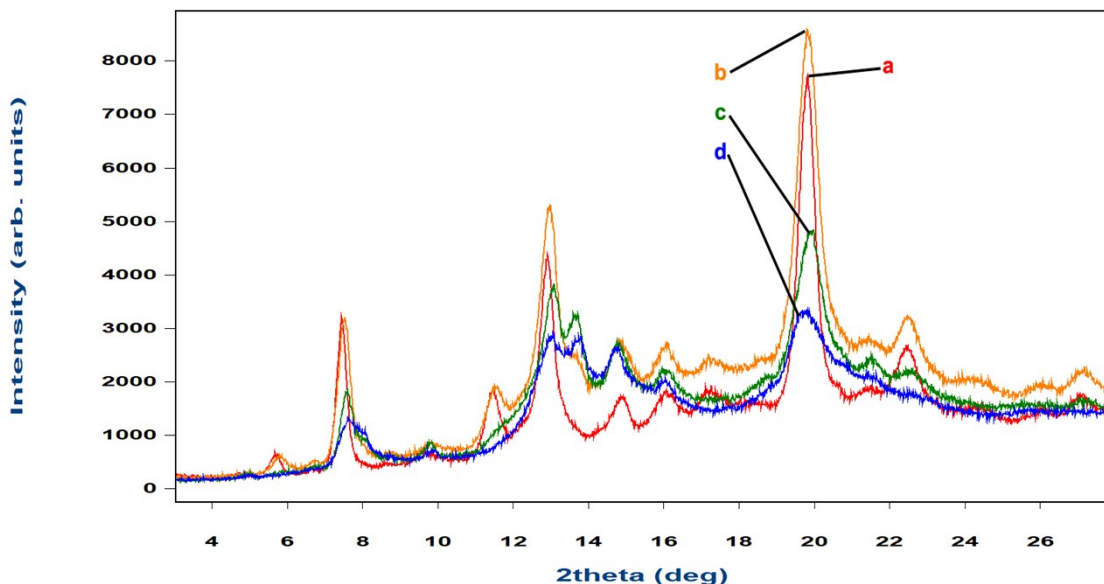
Figure S32. Powder diffractograms for columnar phase of (a) $aCD \cdot 1.3(CH_3)_2CO \cdot 2.7H_2O$ prepared in "hexahydrate+desiccant+guest" system and products of its heating: (b) $aCD \cdot 0.6(CH_3)_2CO \cdot 1.9H_2O$ annealed at 90°C in vacuum; (c) $aCD \cdot 0.3(CH_3)_2CO \cdot 1.6H_2O$ annealed at 120°C in vacuum; (d) $aCD \cdot 0.7H_2O$ annealed at 180°C.
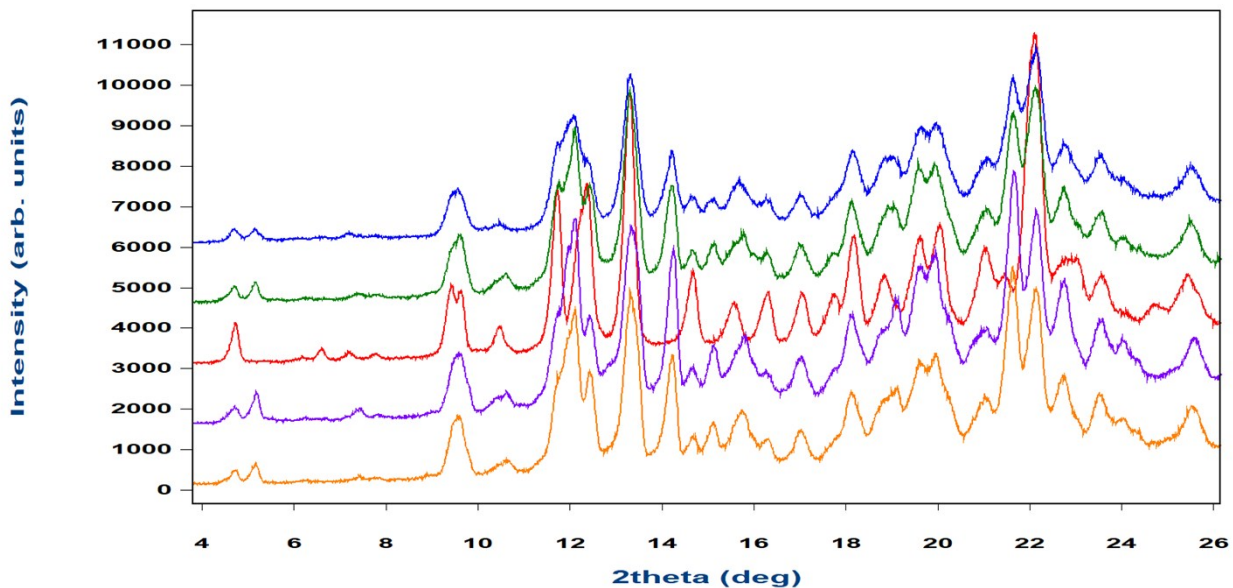
Figure S33. Powder diffractograms of aCD clathrates prepared with saturation of aCD hexahydrate with vapor of: (red) nitromethane; (orange) 1-propanol; (green) propionitrile; (blue) dichloromethane; (violet) acetone. No desiccant was added.

20
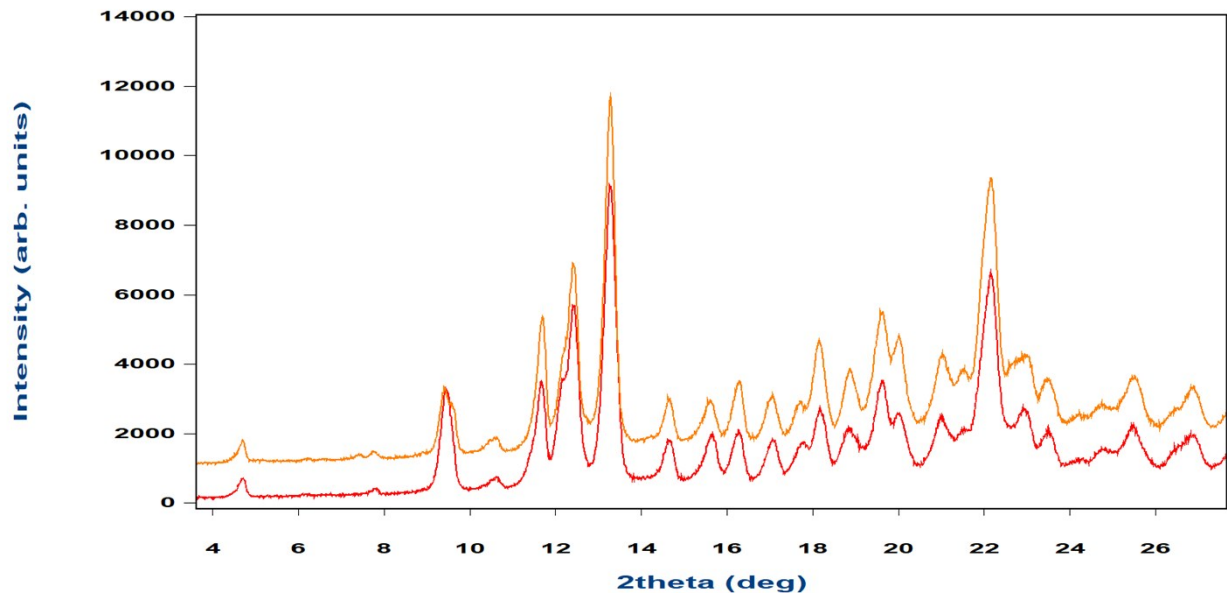
Figure 34. Powder diffractograms of aCD clathrates prepared with saturation of aCD hexahydrate with vapor of: (red) methanol; (orange) ethanol. No desiccant was added.

## Indexation of X-Ray powder diffractogram for anhydrous aCD
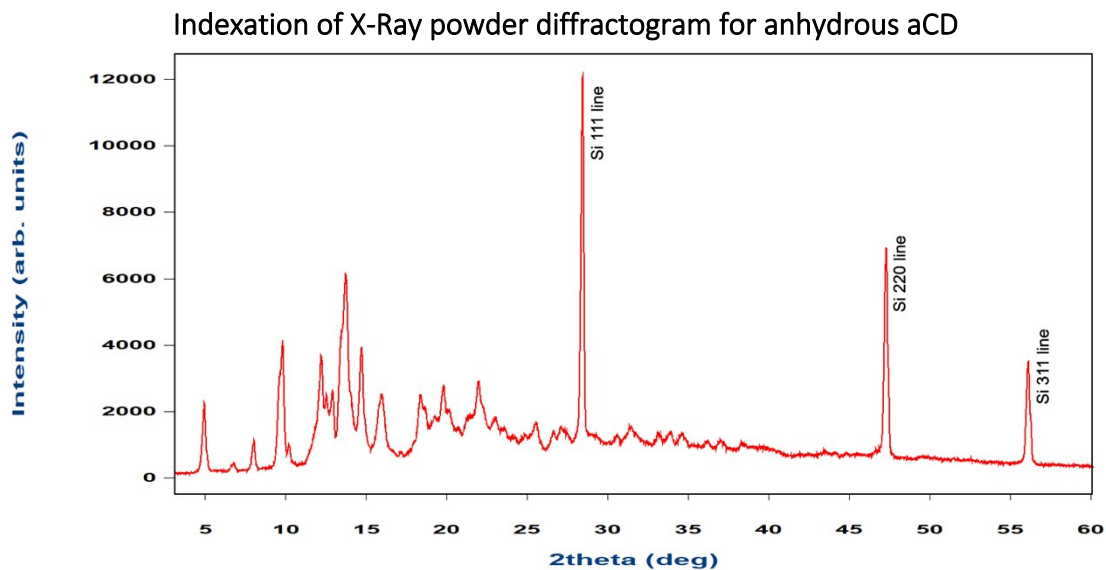
Figure S35. Powder diffractogram of anhydrous aCD[1] with peaks of SRM 640d standard.

Table S5. Unit cell parameters for various forms of aCD*

|	a, Å	b, Å	c, Å	V, Å³
Form IIIa (anhydrous aCD)	14.135	36.030	7.437	3787.41
Form III (aCD·7.57H$_2$O)[2]	14.356	37.538	9.400	5065.62
Form I (aCD·6H$_2$O)[3]	13.700	29.35	11.92	4792.97

* All forms have P2$_1$2$_1$2$_1$ space group.
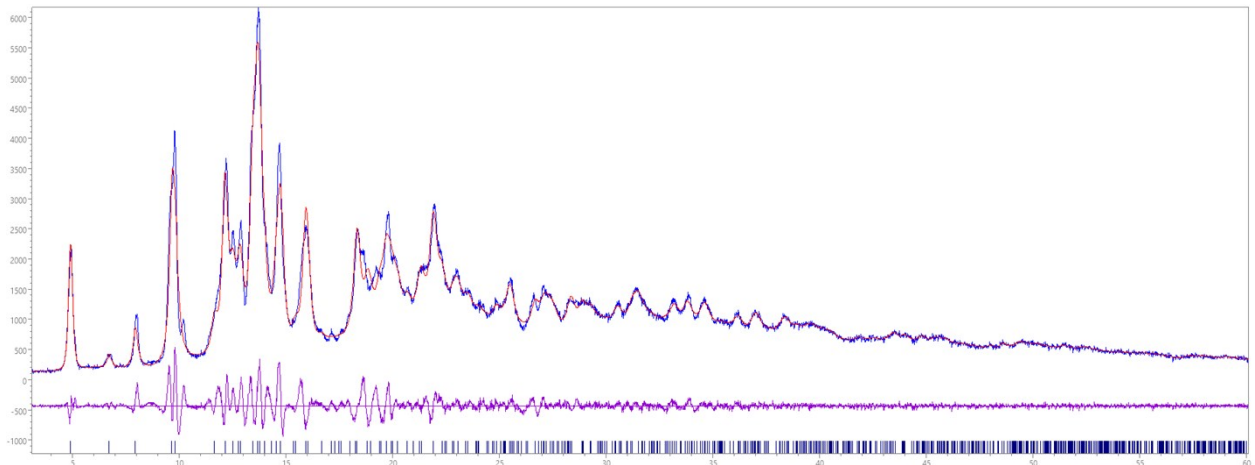
Figure S36. Experimental XRPD pattern (blue), best fit (red) and differential curve (purple) for dried aCD (R_{wp} = 6.781). Blue vertical bars represent Bragg positions for the calculated unit cell and P2$_1$2$_1$2$_1$ space group.

Sorption isotherm data

Table S6. Data on the sorption isotherm of 1-propanol with initially anhydrous aCD for simultaneous sorption of guest and water at constant guest/water molar ratio 1:17.

1-propanol activity, P/P_0	1-propanol inclusion, mol per mol aCD, A	Sorption affinity, $A/(P/P_0)$	aCD hydration, mol water per mol aCD, h	Hydration degree h/h_{max}
0.0001	0.0001	~1	0.1	0.02
0.0007	0.06	81.5	1.0	0.17
0.0014	0.12	84.6	2.1	0.35
0.0220	0.17	7.9	3.0	0.50
0.0194	0.24	12.4	4.2	0.69
0.0415	0.27	6.5	4.7	0.78

Data on kinetics of dehydration for tetrahydrate A

Table S7. Activation energy E_a and logarithm of the pre-exponential factor A for the reaction of aCD dehydration obtained by various approximation methods.

Model	Method	E_a, kJ·mol^{-1}	log A, s^{-1}
-	Friedman	74±11.5	8.51
-	Ozawa-Flynn-Wall	74±9.3	8.59
An, *n*-dimensional nucleation according to Avrami-Erofeev (n=0.58) Corr. coef 0.99915	lin. regr.	79	9.15

Friedman Analysis
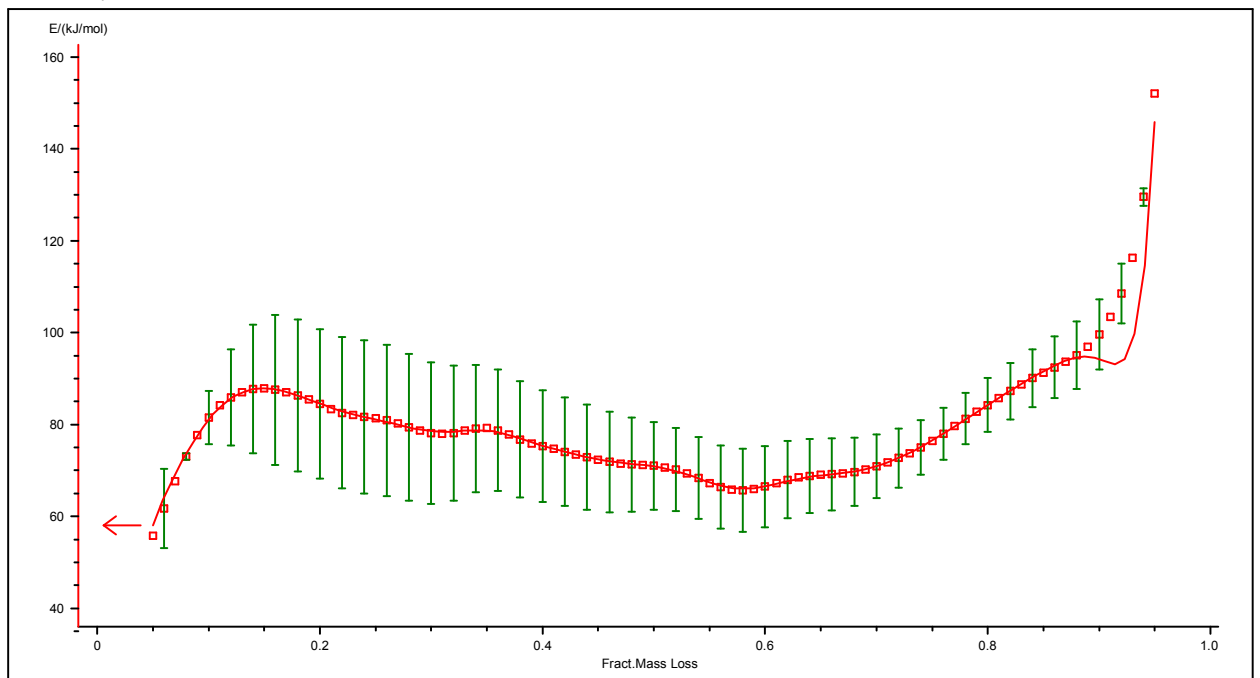
Figure S37. Friedman analysis for the process of the tetrahydrate **A** dehydration.
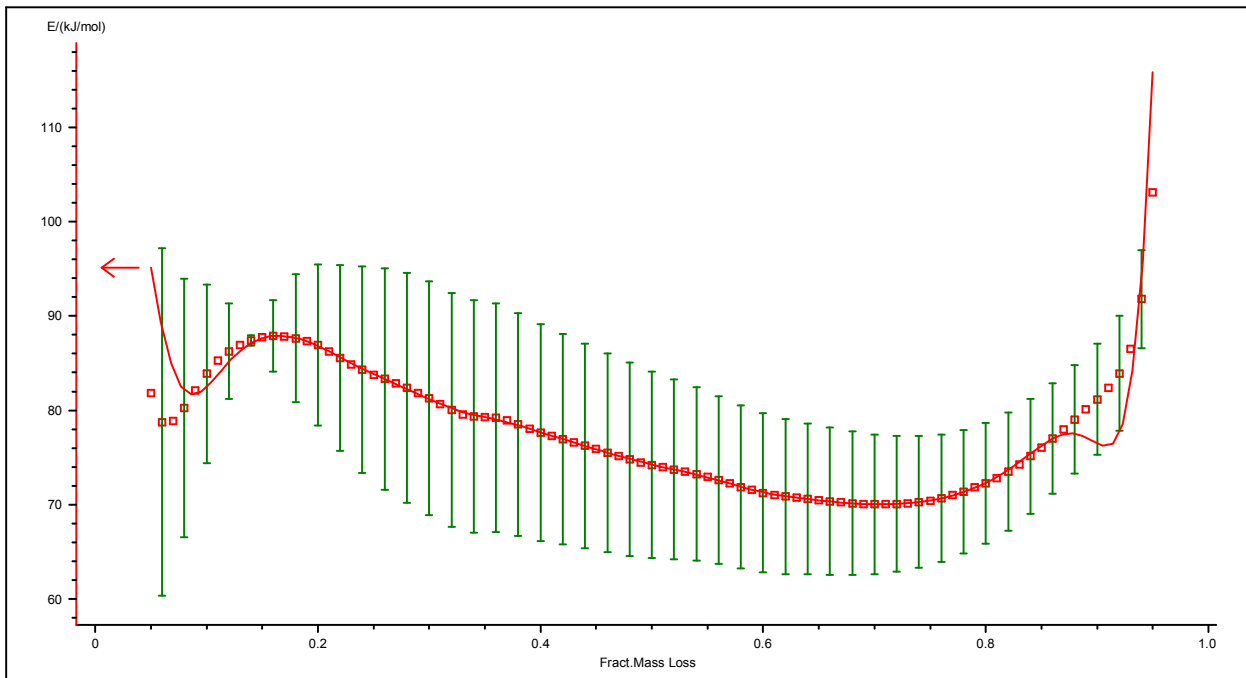
Figure S38. Ozawa-Flynn-Wall analysis for the process of the tetrahydrate **A** dehydration.
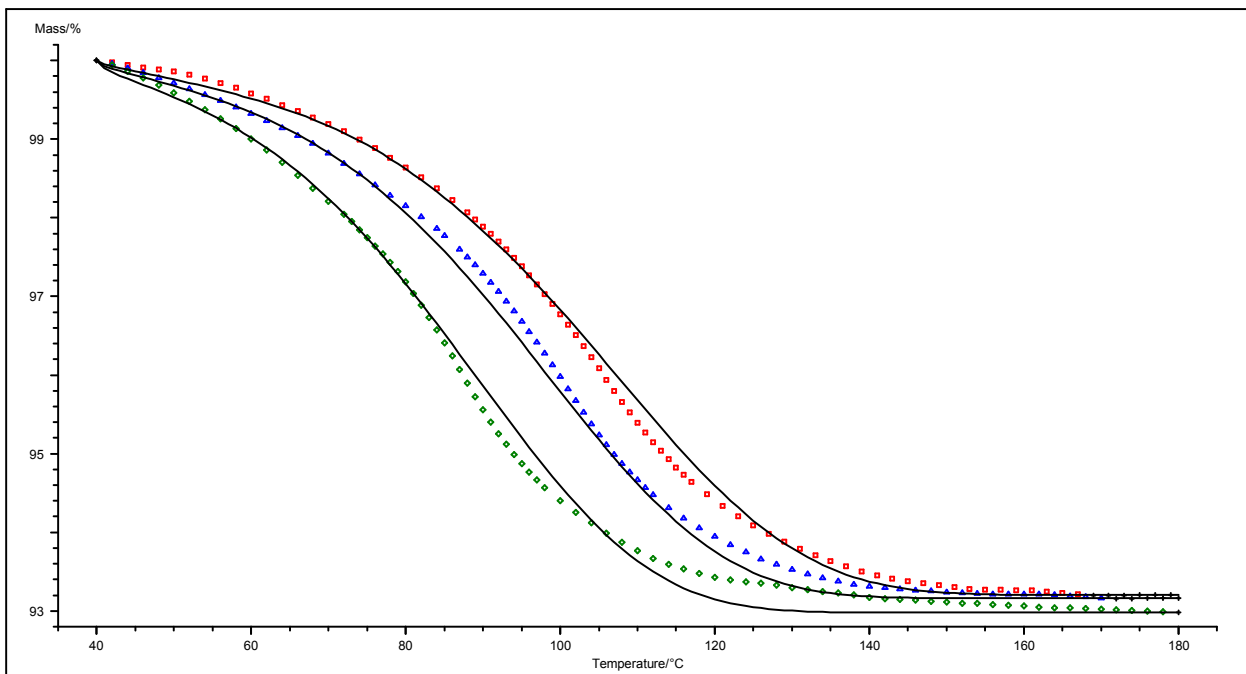
Figure S39. Approximation of TG curves with model method (A_n, n - dimensional nucleation according to Avrami-Erofeev).

Data on kinetics of dehydration for tetrahydrate B

Table S8. Activation energy E_a and logarithm of the pre-exponential factor A for the reaction of aCD dehydration obtained by various approximation methods.

Model	Method	E_a, kJ·mol^{-1}	log A, s^{-1}
-	Friedman	47±15.8	4.34
-	Ozawa-Flynn-Wall	49±12.1	4.60
CnB, reaction of nth order with autocatalysis by product (n=1.39) Corr. coeff. 0.9965	lin. regr.	52	4.99

Friedman Analysis
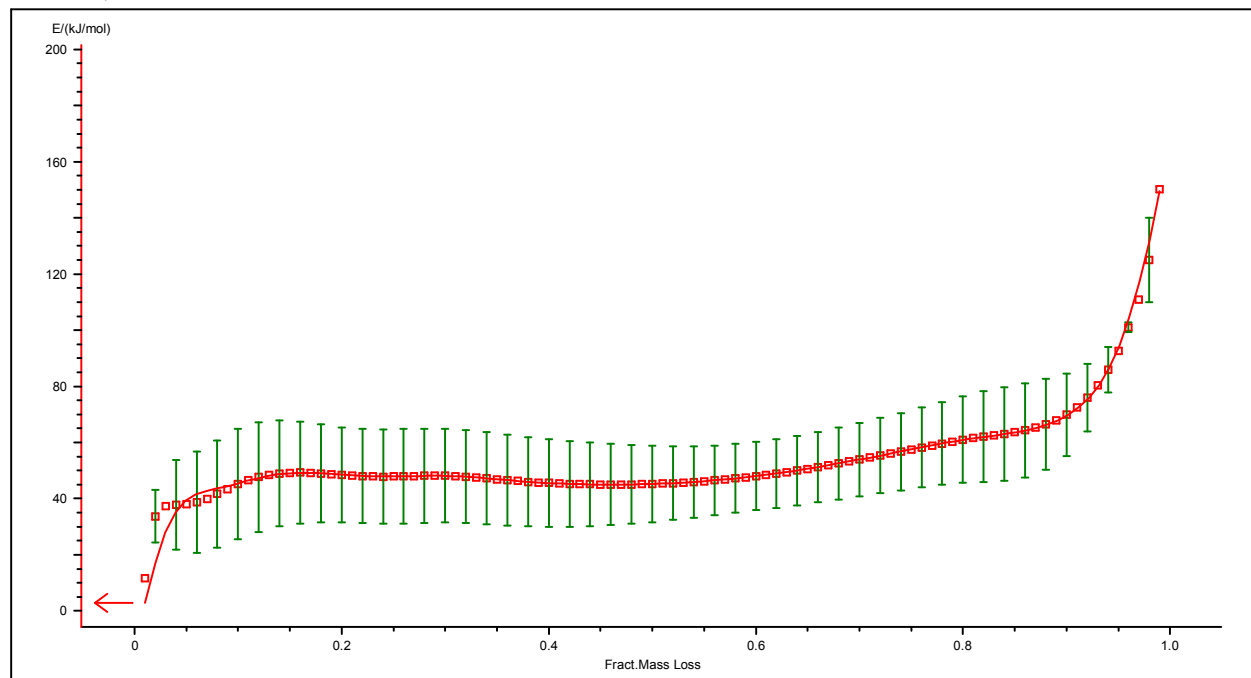
Figure S40. Friedman analysis for the process of the tetrahydrate **B** dehydration.
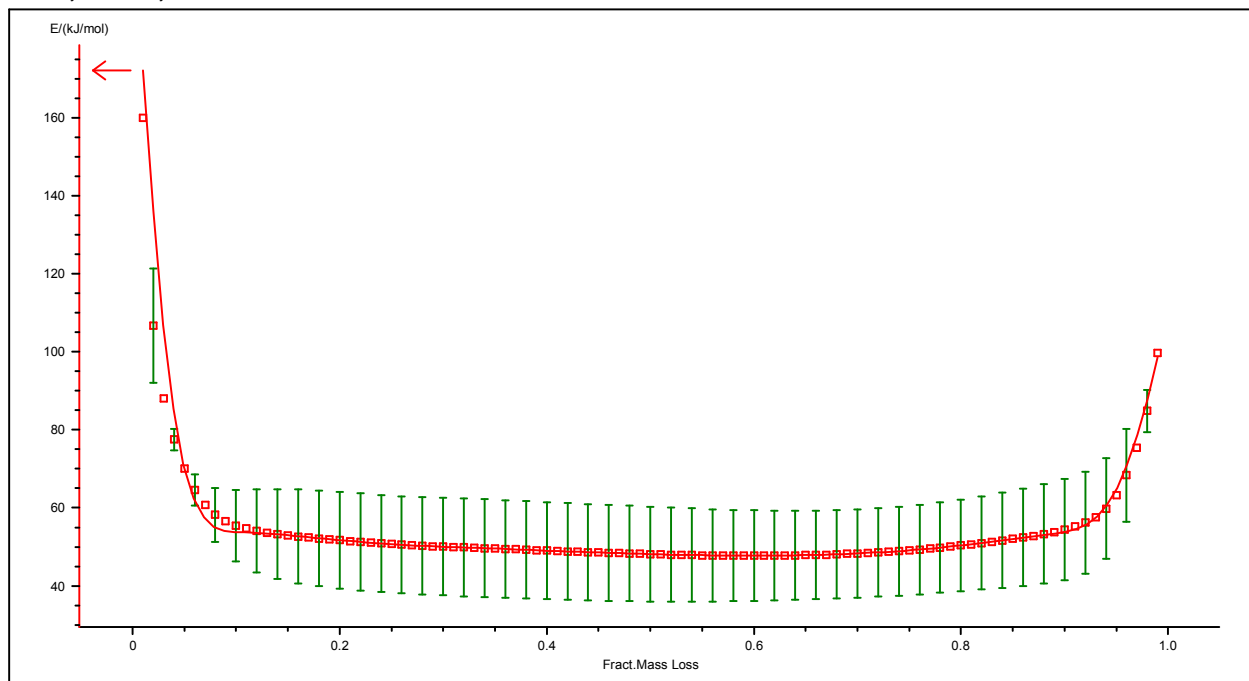
Figure S41. Ozawa-Flynn-Wall analysis for the process of the tetrahydrate **B** dehydration.
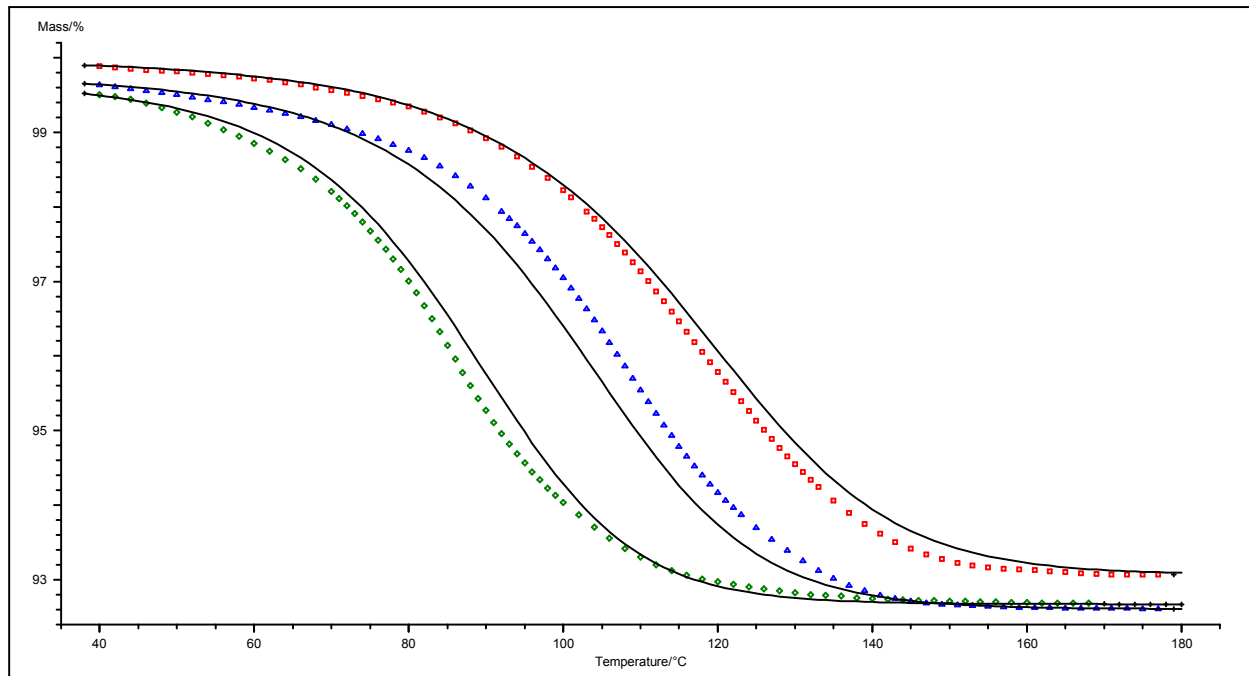
Figure S42. Approximation of TG curves with model method (CnB, n-th order with autocatalysis with product).

Data on kinetics of water and EtCN release from ternary aCD clathrates

Table S9. Activation energy E_a and logarithm of the pre-exponential factor A for the reaction of water removal (1st step of decomposition) from aCD·0.9C_2H_5CN·3.8H_2O prepared from tetrahydrate **A**.

Model	Method	E_a, kJ·mol^{-1}	log A, s^{-1}
-	Friedman	69±16.6	7.78
-	Ozawa-Flynn-Wall	68±7.0	7.58
Fn (reaction of nth order, n=1.72) Corr. coeff. 0.99902	lin. regr.	66	7.40

Table S10. Activation energy E_a and logarithm of the pre-exponential factor A for the reaction of EtCN removal (2nd step of decomposition) from aCD·0.9C_2H_5CN·3.8H_2O prepared from tetrahydrate **A**.

Model	Method	E_a, kJ·mol^{-1}	log A, s^{-1}
-	Friedman	107-159	9.7-15.4
-	Ozawa-Flynn-Wall	106-138	9.8-13.6
D1F, one-dimensional diffusion according to Fick's law Corr. coef 0.9989	lin. regr.	117	9.79

Table S11. Activation energy E_a and logarithm of the pre-exponential factor A for the reaction of water removal (1st step of decomposition) from aCD·1.0C_2H_5CN·4.1H_2O prepared from tetrahydrate **B**.

Model	Method	E_a, kJ·mol^{-1}	log A, s^{-1}
-	Friedman	56±13.4	5.84
-	Ozawa-Flynn-Wall	56±12.2	5.73
CnB, reaction of nth order with autocatalysis by product (n=1.37) Corr. coef 0.9971	lin. regr.	58	5.90

Table S12. Activation energy E_a and logarithm of the pre-exponential factor A for the reaction of EtCN removal (2nd step of decomposition) from aCD·1.0C_2H_5CN·4.1H_2O prepared from tetrahydrate **B**.

| Model	Method	E_a, kJ·mol^{-1}	log A, s^{-1}
-	Friedman	113-171	10.2-16.5
-	Ozawa-Flynn-Wall	90-145	8.3-13.5
An, n-dimensional nucleation according to Avrami-Erofeev (n=0.87) Corr. coef 0.9980	lin. regr.	127	11.9
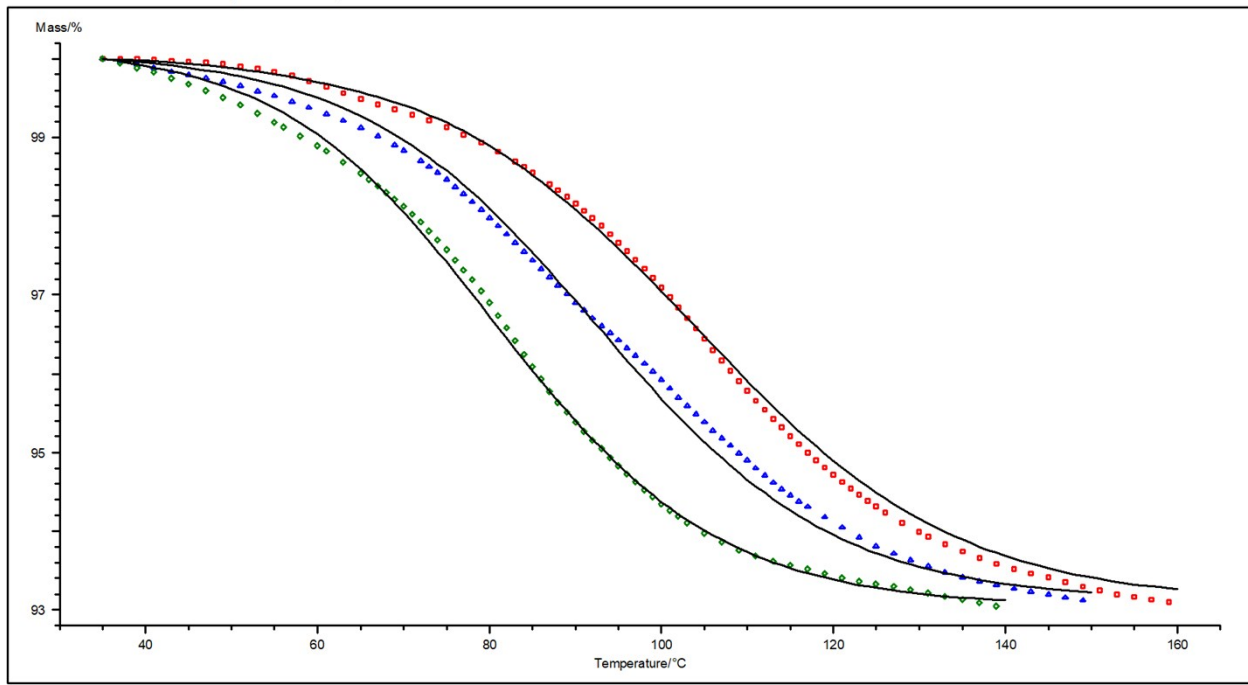
Figure S43. Approximation of TG curves (1 step for aCD·0.9C$_2$H$_5$CN·3.8H$_2$O prepared from tetrahydrate **A**) with model method (Fn).

Friedman Analysis
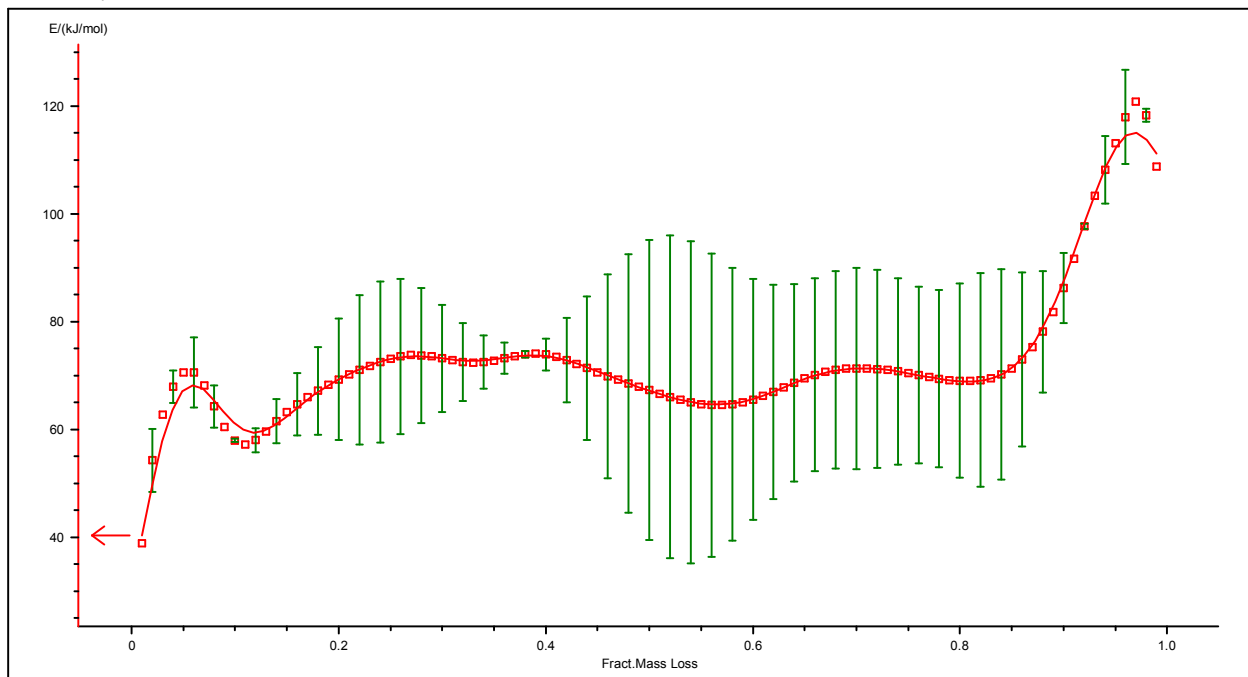
Figure S44. Friedman analysis for the 1 step of decomposition of aCD·0.9C$_2$H$_5$CN·3.8H$_2$O prepared from tetrahydrate **A**

Figure S45. Ozawa-Flynn-Wall analysis for the 1 step of decomposition of aCD·0.9C$_2$H$_5$CN·3.8H$_2$O prepared from tetrahydrate **A**
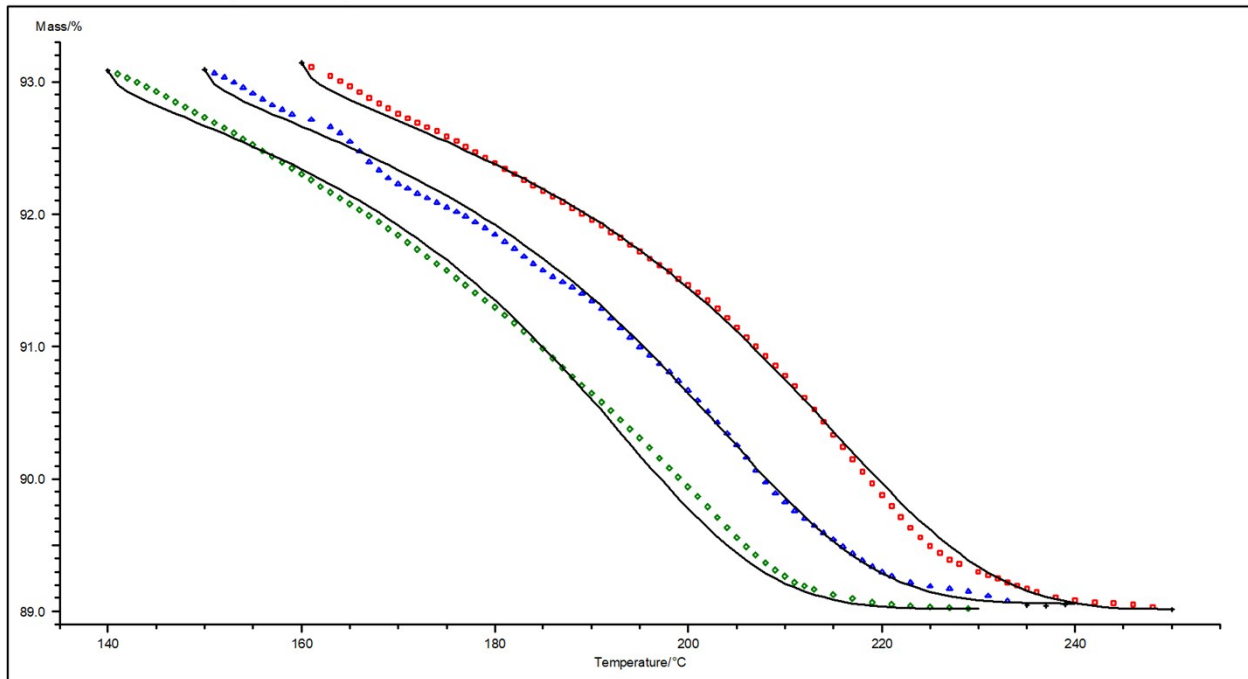
Figure S46. Approximation of TG curves (2nd step for aCD·0.9C$_2$H$_5$CN·3.8H$_2$O prepared from tetrahydrate **A**) with model method (D1F).

Friedman Analysis
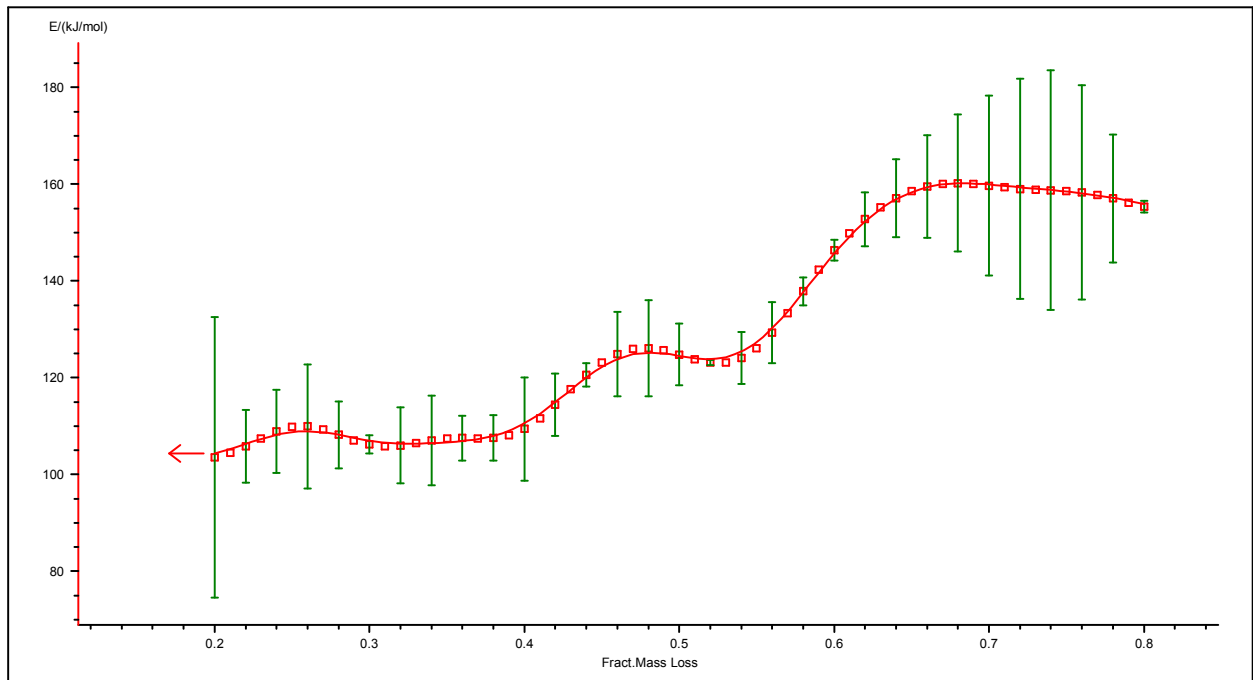
Figure S47. Friedman analysis for the 2nd step of decomposition of aCD·0.9C$_2$H$_5$CN·3.8H$_2$O prepared from tetrahydrate **A**

Ozawa-Flynn-Wall Analysis
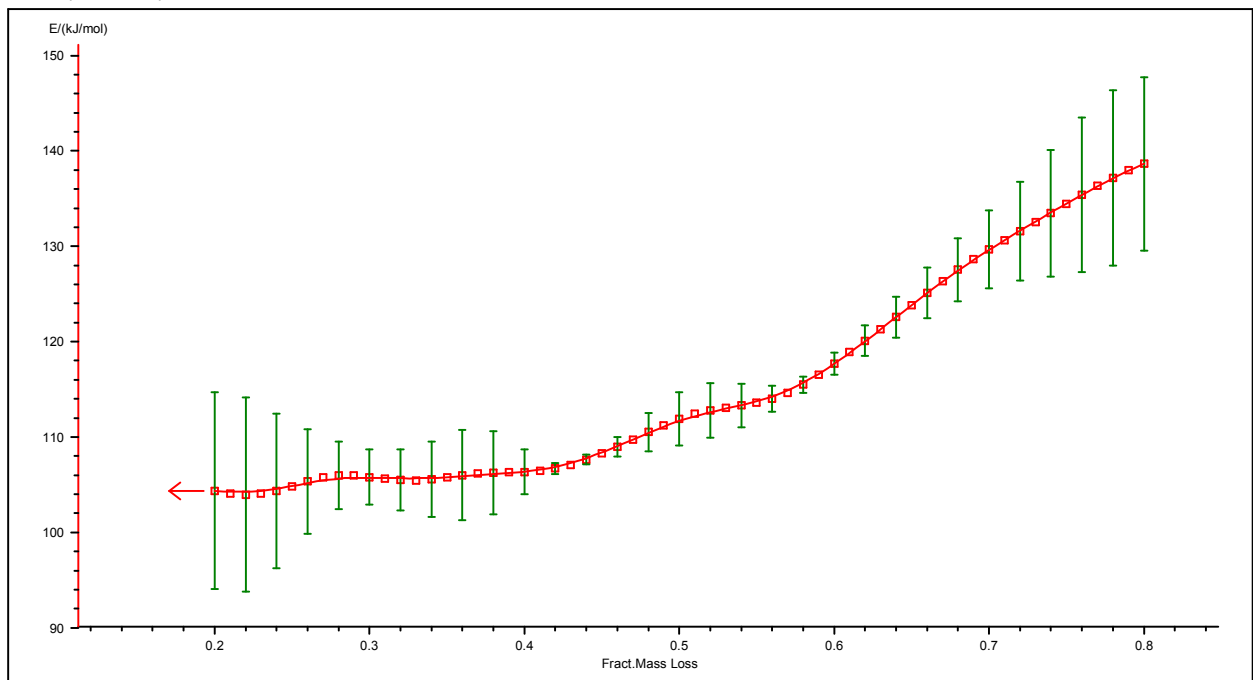
Figure S48. Ozawa-Flynn-Wall analysis for the 2nd step of decomposition of aCD·0.9C$_2$H$_5$CN·3.8H$_2$O prepared from tetrahydrate **A**
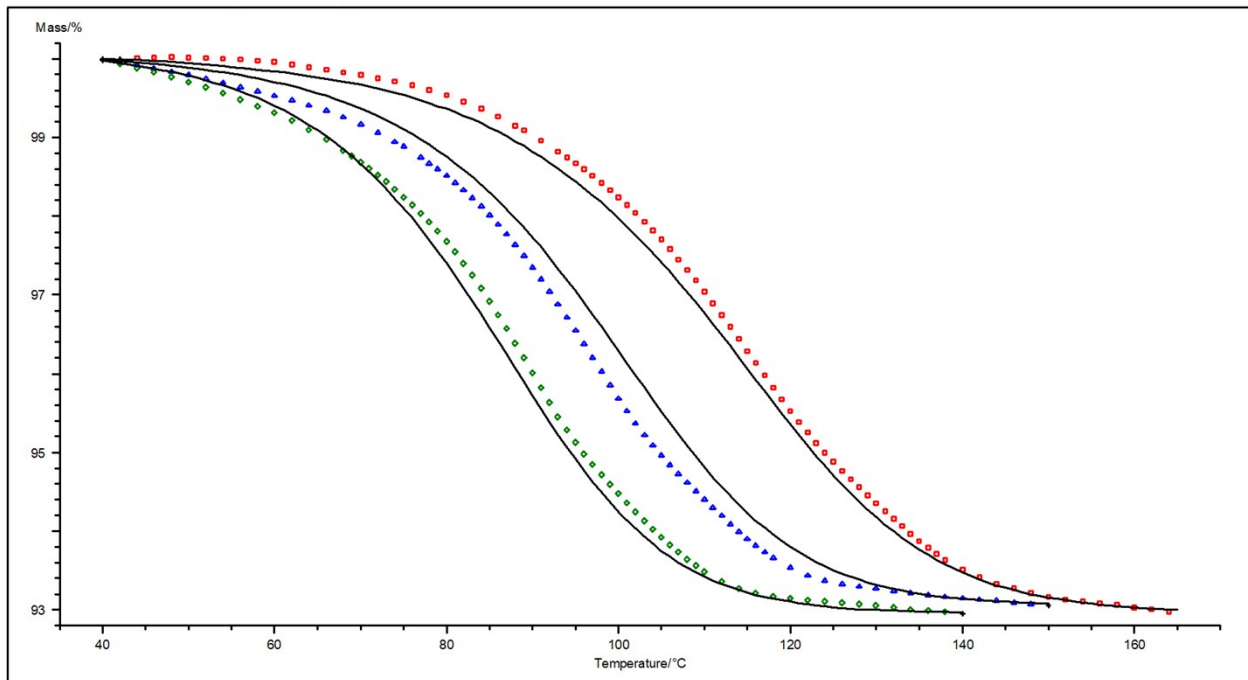
Figure S49. Approximation of TG curves (1st step for $aCD \cdot 1.0C_2H_5CN \cdot 4.1H_2O$ prepared from tetrahydrate **B**) with model method (CnB).
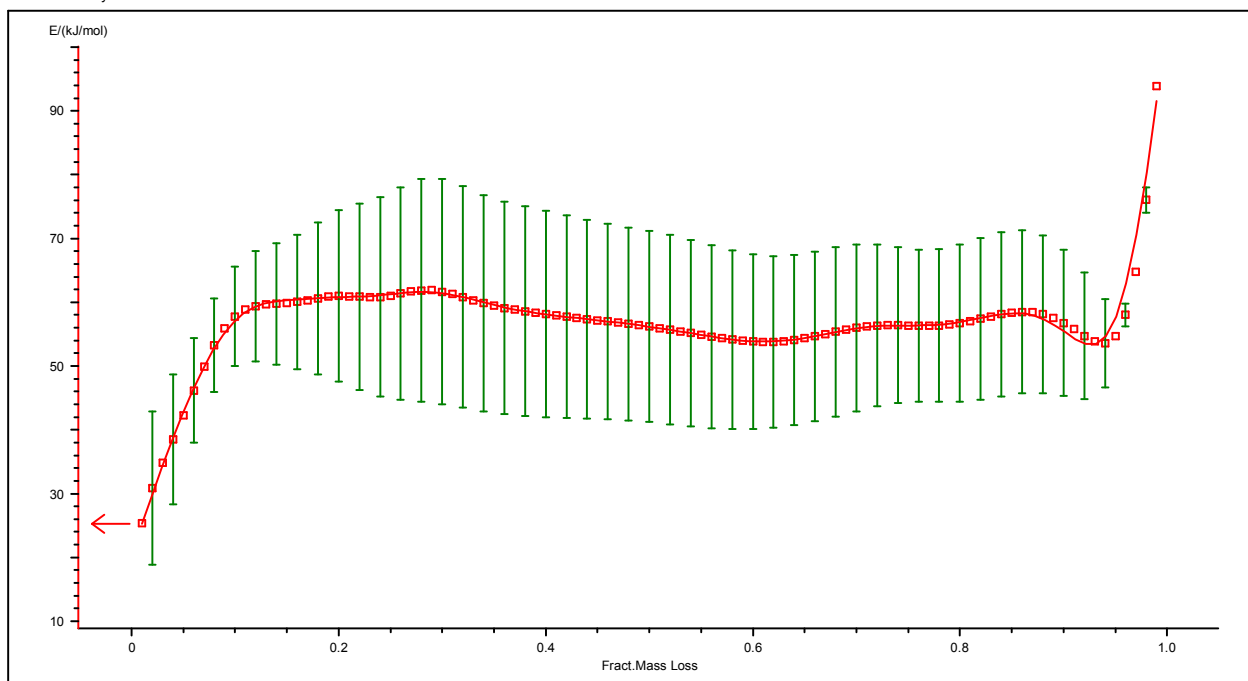

Figure S50. Friedman analysis for the 1 step of decomposition of $aCD \cdot 1.0C_2H_5CN \cdot 4.1H_2O$ prepared from tetrahydrate **B**.

Figure S51. Ozawa-Flynn-Wall analysis for the 1 step of decomposition of aCD·1.0C$_2$H$_5$CN·4.1H$_2$O prepared from tetrahydrate **B**.
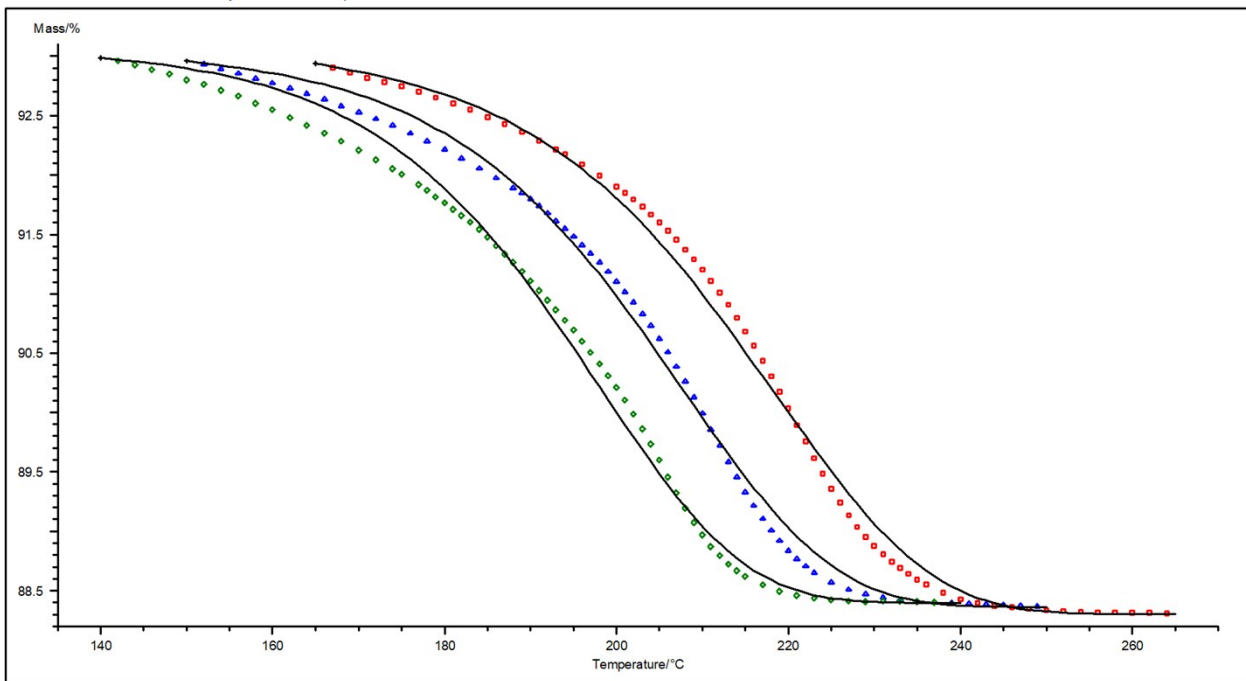
Figure S52. Approximation of TG curves (2nd step for aCD·1.0C$_2$H$_5$CN·4.1H$_2$O prepared from tetrahydrate **B**) with model method (An).

Friedman Analysis
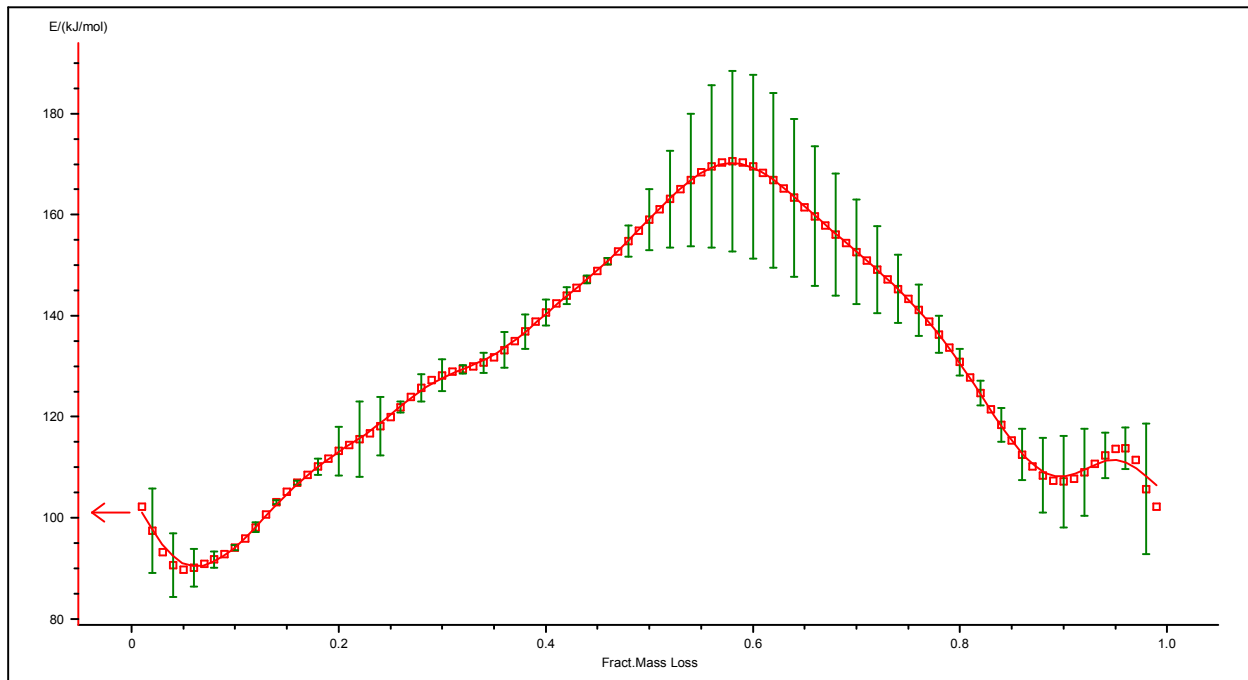
Figure S53. Friedman analysis for the 2nd step of decomposition of aCD·1.0C$_2$H$_5$CN·4.1H$_2$O prepared from tetrahydrate **B**.

Ozawa-Flynn-Wall Analysis
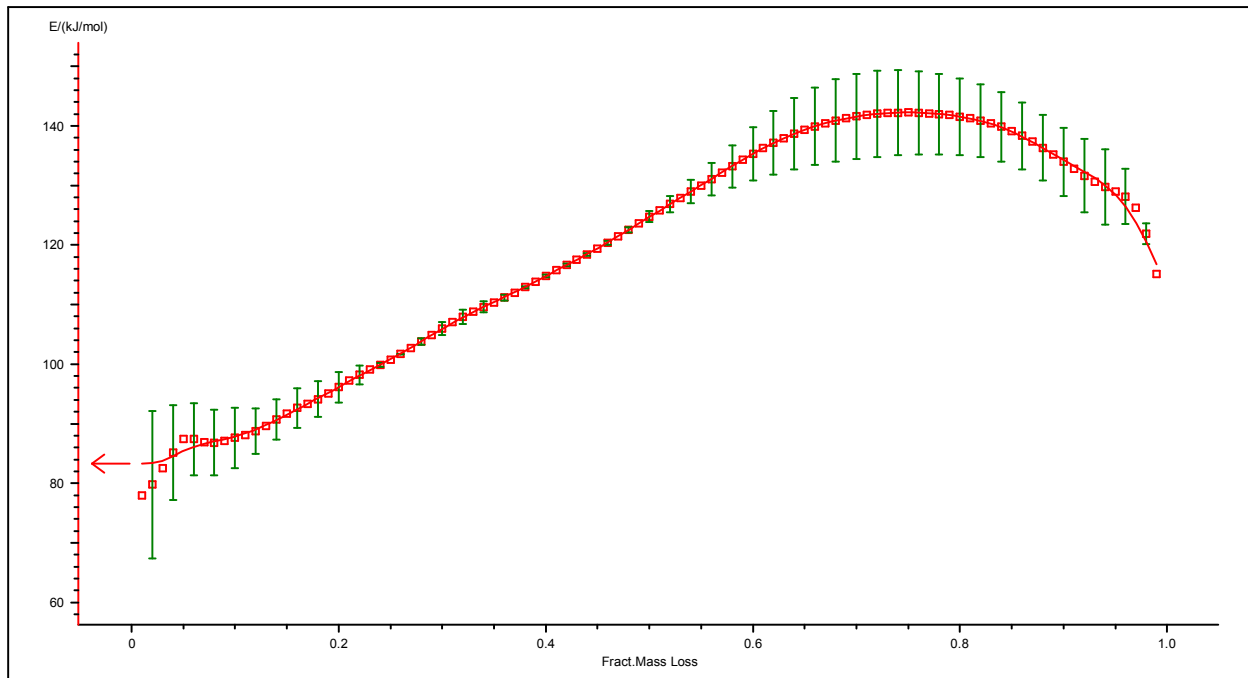
Figure S54. Ozawa-Flynn-Wall analysis for the 2nd step of decomposition of aCD·1.0C$_2$H$_5$CN·4.1H$_2$O prepared from tetrahydrate **B**.

References

1. A. K. Gatiatulin, V. Y. Osel'skaya, M. A. Ziganshin and V. V. Gorbatchuk, Size exclusion effect in binary inclusion compounds of α-cyclodextrin, Phys. Chem. Chem. Phys., 2018, 20, 26105–26116. **DOI: 10.1039/c8cp03104e**
2. K. K. Chacko and W. Saenger, Topography of cyclodextrin inclusion complexes. 15. Crystal and molecular structure of the cyclohexaamylose-7.57 water complex, form III. Four- and six-membered circular hydrogen bonds, J. Am. Chem. Soc., 1981, 103, 1708–1715. **DOI: 10.1021/ja00397a021**
3. K. Lindner and W. Saenger, Topography of cyclodextrin inclusion complexes. XVI. Cyclic system of hydrogen bonds: structure of α-cyclodextrin hexahydrate, form (II): comparison with form (I), Acta Crystallogr. Sect. B Struct. Crystallogr. Cryst. Chem., 1982, 38, 203–210. **DOI: 10.1107/S0567740882002386**